Published in final edited form as:
Dalton Trans. 2011 June 21; 40(23): 6168–6195. doi:10.1039/c0dt01595d.

A practical guide to the construction of radiometallated bioconjugates for positron emission tomography

Brian M. Zeglis and **Jason S. Lewis**
Department of Radiology and Program in Molecular Pharmacology and Chemistry Memorial Sloan-Kettering Cancer Center, New York, NY 10021, USA. Fax: (646)-888-3039; Tel: (646)-888-3038

Jason S. Lewis: lewisj2@mskcc.org

Abstract

Positron emission tomography (PET) has become a vital imaging modality in the diagnosis and treatment of disease, most notably cancer. A wide array of small molecule PET radiotracers have been developed that employ the short half-life radionuclides ^{11}C, ^{13}N, ^{15}O, and ^{18}F. However, PET radiopharmaceuticals based on biomolecular targeting vectors have been the subject of dramatically increased research in both the laboratory and the clinic. Typically based on antibodies, oligopeptides, or oligonucleotides, these tracers have longer biological half-lives than their small molecule counterparts and thus require labeling with radionuclides with longer, complementary radioactive half-lives, such as the metallic isotopes ^{64}Cu, ^{68}Ga, ^{86}Y, and ^{89}Zr. Each bioconjugate radiopharmaceutical has four component parts: biomolecular vector, radiometal, chelator, and covalent link between chelator and biomolecule. With the exception of the radiometal, a tremendous variety of choices exists for each of these pieces, and a plethora of different chelation, conjugation, and radiometallation strategies have been utilized to create agents ranging from ^{68}Ga-labeled pentapeptides to ^{89}Zr-labeled monoclonal antibodies. Herein, the authors present a practical guide to the construction of radiometal-based PET bioconjugates, in which the design choices and synthetic details of a wide range of biomolecular tracers from the literature are collected in a single reference. In assembling this information, the authors hope both to illuminate the diverse methods employed in the synthesis of these agents and also to create a useful reference for molecular imaging researchers both experienced and new to the field.

Introduction

Over the course of the past fifty years, advances in medical imaging have revolutionized clinical practice, with a wide variety of imaging modalities playing critical roles in the diagnosis and treatment of disease. Today, clinicians have at their disposal a remarkable range of medical imaging techniques, from more conventional modalities like ultrasound, conventional radiography (X-rays), X-ray computed tomography (CT scans), and magnetic resonance imaging (MRI) to more specialized methodologies such as single-photon emission computed tomography (SPECT) and positron emission tomography (PET).

In recent years, medical imaging research has experienced a paradigm shift from its foundations in anatomical imaging towards techniques aimed at probing tissue phenotype and function.[1] Indeed, both the cellular expression of disease biomarkers and fluctuations in tissue metabolism and microenvironment have emerged as extremely promising targets for

Correspondence to: Jason S. Lewis, lewisj2@mskcc.org.

imaging.[2] Without question, the unique properties of radiopharmaceuticals have given nuclear imaging a leading role in this movement. The remarkable sensitivity of PET and SPECT combines with their ability to provide information complementary to the anatomical images produced by other modalities to make these techniques ideal for imaging biomarker- and microenvironment-targeted tracers.[3,4] Both relatively young modalities, SPECT and PET have had an impact on medicine (and oncology in particular), which belies their novelty, and both have been the topic of numerous thorough and well-reasoned reviews.[5–9] Both modalities have become extremely important in the clinic, and while PET is generally more expensive on both the clinical and pre-clinical levels, it also undoubtedly possesses a number of significant advantages over its single-photon cousin, most notably the ability to quantify images, higher sensitivity (PET requires tracer concentrations of $\sim 10^{-8}$ to 10^{-10} M, while SPECT requires concentrations approaching 10^{-6} M), and higher resolution (typically 6–8 mm for SPECT, compared to 2–3 mm or lower for PET). Therefore, in the interest of scope, the article at hand will limit itself to the younger and higher resolution of the techniques: positron emission tomography.

Regardless of the broader perspective, any discussion of PET benefits from a brief description of the underlying physical phenomena. Starting from the beginning, a positron released by a decaying radionuclide will travel in a tissue until it has exhausted its kinetic energy. At this point, it will encounter its antiparticle, an electron, and the two will mutually annihilate, completely converting their mass into two 511 keV γ-rays that must, due to conservation of momentum, have equal energies and travel 180° relative to one another. These γ-rays will then leave the tissue and strike waiting coincidence detectors; importantly, only when signals from two coincidence detectors simultaneously trigger the circuit is an output generated. The two principal advantages of PET thus lie in the physics: the short initial range of the positrons results in high resolution, and the coincidence detection methodology allows for tremendous sensitivity.

In the early 1950s, Brownell[10] and Sweet[11] developed the first devices for creating images using the coincident detection of γ-rays emitted from positron-electron annihilation events. At the same time, these researchers and others were pioneering the oncologic applications of positron imaging, specifically the imaging of brain tumors.[10–14] Not until the 1970s, however, did the field take the next important practical step forward: tomographic systems and computer analysis were first applied to positron imaging, innovations which paved the way for the widespread clinical use of the modality.

Since the advent of PET in both the clinic and medical research laboratories, a number of positron-emitting isotopes have been developed for use in radiopharmaceuticals. For years, the field was dominated by small molecule tracers, radiopharmaceuticals whose short biological half-lives favor the use of non-metallic radionuclides with correspondingly short radioactive half-lives, such as ^{18}F, ^{15}O, ^{13}N, and ^{11}C (Table 1). In many ways, this is still true: [^{18}F]-fluoride and the ubiquitous [^{18}F]-fluorodeoxyglucose ([^{18}F]-FDG) are the only FDA-approved PET radiopharmaceuticals commonly employed in oncology ([^{13}N]-NH_3 and [^{82}Rb]-RbCl are FDA-approved but are used principally for myocardial perfusion scans). Further still, an examination of the list of PET radiotracers currently in NIH-sponsored clinical trials reveals an overwhelming majority of agents with non-metallic radionuclides, including among others the promising agents [^{18}F]-FLT, [^{18}F]-FES, [^{18}F]-FDHT, [^{18}F]-FMISO, [^{18}F]-FACBC, [^{18}F]-fluoroethylcholine, [^{18}F]-deshydroxycholine, [^{18}F]-FMAU, [^{11}C]-acetate, [^{11}C]-choline, [^{11}C]-MeAIB, [^{11}C]-MET, [^{124}I]-IAZGP, and [^{124}I]-FIAU.[15]

Yet despite the significant successes of small molecule probes labeled with non-metallic isotopes, these radionuclides possess a few critical limitations. First, the short half-lives of

the most common non-metallic radionuclides - approximately 20 min for ^{11}C, 10 min for ^{13}N, 2 min for ^{15}O, and 110 min for ^{18}F - allow only for investigations of biological processes on the order of minutes or a few hours using tracers with rapid pharmacokinetic profiles. Second, both the short half-lives of the radionuclides and the frequent necessity of incorporating the radioisotopes into the core structure of the tracer (rather than in an appended chelator or prosthetic group) often necessitate demanding and complex syntheses. Third, the clinical and pre-clinical use of short half-life, non-metallic radionuclides often requires a local cyclotron facility; in its absence, the radionuclide in question will undergo many half-lives of decay while in transit. Given the resources required for the construction and operation of medical cyclotrons, this is simply not an option in many locations.

These limitations have been brought into focus by the increasing study and development of biomolecular targeting agents for cancer, including short peptides, antibodies, antibody fragments, and natural and non-natural oligonucleotides. Given that Nature herself has designed or inspired these agents, they often show sensitivities and specificities for cancer cell biomarkers that far exceed those of their small molecule counterparts. However, these biomolecular tracers typically have biological half-lives that are much longer than the radioactive half-lives of the most common non-metallic positron-emitting radionuclides; further, though less pressing, many of these biomolecules are incompatible with the chemistry required for direct labeling with non-metallic radionuclides.[16–19]

Given the enormous potential of biomolecular imaging agents, significant effort has been dedicated to the production, purification, and radiochemistry of positron-emitting radioisotopes of the metals Zr, Y, Ga, and Cu. These isotopes, specifically ^{64}Cu, ^{68}Ga, ^{86}Y, and ^{89}Zr, have radioactive half-lives (roughly 12.7, 1.1, 14.7, and 78.4 h, respectively) that favorably complement the biological half-lives of many biomolecular targeting vectors (Table 2). Although all four radiometals emit positrons, each has a characteristic positron range, which is the principal factor in determining imaging resolution. ^{64}Cu and ^{89}Zr emit very low energy positrons, producing image resolution comparable to that of ^{18}F. ^{86}Y and ^{68}Ga, in contrast, emit higher energy positrons, which can result in slightly lower imaging resolutions, though this can be corrected through the use of mathematical algorithms.[20] Further still, and equally critical, all four metals form stable chelate complexes that may be employed for the radiolabeling of biomacromolecules. To be sure, not all biomolecular PET tracers are labeled with radiometals, nor are all radiometallated PET tracers biomolecules. An ^{18}F-labeled variant of the integrin-targeting RGD peptide[21] and an ^{124}I-labeled carbonic anhydrase-targeting antibody[22] have produced very exciting results and are currently being employed in human studies. Moreover, a few radiometal-based small molecule tracers have also proved extremely promising, most notably [^{64}Cu]-Cu(PTSM)[23] and [^{64}Cu]-Cu(ATSM),[24] with the latter currently in a multi-center clinical trial as an imaging agent for hypoxia.[25–28] Yet, despite these exceptions, the single most important application of positron-emitting radiometals is the development of tracers based on peptides, antibodies, and oligonucleotides.

Importantly, the basic strategy for the incorporation of a radiometal into a biomolecule differs somewhat from the synthesis of a small molecule radiotracer containing a non-metallic PET radionuclide. In small molecule tracers, the radionuclide most often replaces an isotopologue (*e.g.* [^{11}C]-acetate or [^{15}O]-H_2O) or is incorporated into the basic structure of a molecule with either the intent of strategically altering the behavior of the parent molecule (*e.g.* [^{18}F]-FDG) or, more likely, disturbing the activity of the parent molecule as little as possible (*e.g.* [^{18}F]-FDHT or [^{18}F]-FES). In contrast, in biomolecular tracers, the radiometal is almost never directly attached to the biomolecule itself. Rather, the radionuclide is bound to a chelating moiety (*e.g.* DOTA[29] or EDTA[30]), which is first

covalently appended to the biomolecule with the intent of altering the vector's biochemical properties as little as possible.[31,32]

As new targets are described and radiometals become more available to the wider molecular imaging community, the amount of research into radiometal-based PET tracers has exploded in recent years. For example, over 60% of all publications describing ^{89}Zr-PET have been published in the last four years (with well over 20% in 2010 alone).[33] Indeed, the dramatic growth in this area and the expansion in the availability of radiometals have had the dual effects of broadening the appeal of biomolecular PET imaging and opening the field to investigators who previously may have left the development of PET probes to dedicated radiochemistry and molecular imaging laboratories. However, the frenetic pace of the field and the array of choices in chelation, conjugation, and metallation strategies may serve as an obstacle to those who are interested in the development of radiometallated PET tracers but lack significant bioconjugation or radiochemical experience.

This perspective aims at lowering this barrier. Here, we strive to create a practical guide to the synthesis of radiometal-based PET tracers. To this end, we have compiled the experimental details of chelator choice, conjugation strategy, and radiometallation conditions from the syntheses of a wide array of ^{64}Cu-, ^{68}Ga-, ^{86}Y-, and ^{89}Zr-labeled PET agents. Typically, reviews discuss the structure, behavior, biology, and imaging applications of these agents, with the experimental details touched upon only briefly or simply referenced.[7,16,34–37] All too often, however, the search for a specific conjugation or metallation protocol results in an elongated, and in some cases circuitous, trek through the literature to find a simple incubation time or buffer concentration. Importantly, we do not strive for an exhaustive review of the radiochemistry or imaging applications of radiometal-based PET tracers. Others - most notably Carolyn Anderson and her coworkers at the Washington University School of Medicine and Martin Brechbiel and his coworkers at the National Cancer Institute - have produced well-written and remarkably thorough reviews on these topics.[3,30,34,38–45]

The core of this perspective lies not in the text but rather in the series of tables containing the practical details of chelator conjugation and radiometallation from a diverse collection of ^{64}Cu-, ^{68}Ga-, ^{86}Y-, and ^{89}Zr-labeled bioconjugates. We have elected not to include two types of macromolecular radiopharmaceuticals, bispecific antibodies and biomolecule-based nanoparticles, in the interest of space and scope, though these have been addressed well elsewhere.[46–49] Further, it is important to note that some of the conjugation strategies described herein are now, for the most part, obsolete with respect to their original vector; for example, a number of syntheses for DOTATOC will be outlined, though this DOTA-modified somatostatin analogue is now widely commercially available. Yet we believe it is important to detail these conjugation methods nonetheless, for the synthetic routes themselves may prove useful in the future for the creation of conjugates with different biomolecular vectors. In collecting these techniques in one place, we hope not only to shed light upon the diverse methods employed in the synthesis of these agents but also, and perhaps more importantly, to create a useful reference for both experienced molecular imaging scientists and researchers new to the field.

The anatomy of a PET bioconjugate

A radiometallated PET bioconjugate has four component parts, each of which must be carefully considered during the design and synthesis of the tracer: (1) the biomolecular targeting vector, (2) the radiometal, (3) the chelator, and (4) the linker connecting the chelator and the biomolecule (Fig. 1). A detailed discussion of the possible targeting vectors lies outside the scope of this work, though biomolecules ranging from cyclic pentapeptides and short oligonucleotides to 40-amino acid peptides, antibody fragments, and full

antibodies have been employed.[30] Of course, the most important facet of the biomolecule moiety is its specificity for its biomarker target. Indeed, a wide array of biomarkers have been exploited. Most often, the chosen target is a cell surface marker protein or receptor, such as the somatostatin receptor family (SSTr),[50] integrin family (*e.g.* $\alpha_v\beta_3$),[51] gastrin-releasing peptide receptor (GRPR),[52] and epidermal growth factor receptor (EGFR).[53] In more specialized cases, disialogangliosides (*e.g.* GD2), mRNA gene products, and even the low pH environment of tumors have been targeted by antibodies,[54] oligonucleotides,[55] and short peptides,[56] respectively. Targeting cytosolic proteins and enzymes with antibodies and oligopeptides is rare due to the considerable difficulty of getting large biomolecules into the cytoplasm. However, significant progress is being made in the development of cell- and nucleus-penetration strategies, and this technology may prove productive for intracellular or intranuclear PET imaging agents in the near future.

Radiometals: properties and production

The principal radiometals employed for the labeling of biomolecular tracers are ^{64}Cu, ^{68}Ga, ^{86}Y, and ^{89}Zr. Of course, these are not the only positron-emitting radiometals. Some metallic radioisotopes, such as ^{60}Cu, ^{61}Cu, ^{62}Cu, ^{82}Rb, ^{52m}Mn, and ^{94m}Tc, have been used in PET studies to varying degrees, but their half-lives make them far better suited for small molecule tracers (*e.g.* [^{60}Cu]-Cu(ATSM)).[57–60] Other positron-emitting radiometals, including ^{45}Ti ([^{45}Ti]-transferrin[61]), ^{52}Fe ([^{52}Fe]-citrate/transferrin[62]), ^{55}Co ([^{55}Co]-antiCEA F(ab′)$_2$[63,64]), ^{66}Ga ([^{66}Ga]-octreotate[65]), ^{110m}In ([^{110m}In]-octreotate[66]), and ^{74}As ([^{74}As]-bavituximab[67,68]), have been employed in the synthesis of biomolecular radiopharmaceuticals.[41] However, these will not receive more than a brief discussion here, due to either the lack of more than one or two radiotracers per isotope, the limited availability of the radionuclide in question, or decay characteristics that make the isotope sub-optimal for use in a clinical PET radiopharmaceutical.[40]

The selection of a radiometal from the four main candidates, ^{64}Cu, ^{68}Ga, ^{86}Y, and ^{89}Zr, is a critical factor in determining the ultimate properties of a PET bioconjugate. In this regard, one of the most important considerations is matching the radioactive half-life of the isotope to the biological half-life of the biomolecule. For example, ^{68}Ga is an inappropriate choice for labeling fully intact IgG molecules, for the radionuclide will decay through a number of half-lives before the antibody reaches its fully optimal biodistribution within the body. Therefore, the longer lived radiometals ^{64}Cu, ^{86}Y, and especially ^{89}Zr are most often employed for immunoPET with fully intact mAbs. That said, ^{68}Ga has been used successfully in the construction of PET bioconjugates based on antibody fragments with shorter biological half-lives. Conversely, ^{89}Zr would be an inappropriate choice for a short peptide radiotracer; in this case, the multi-day radioactive half-life of ^{89}Zr would far exceed what is typically a multi-hour biological half-life of the peptide, resulting in poor PET counting statistics and unnecessarily increased radiation dose to the patient. Thus, ^{64}Cu, ^{86}Y, and ^{68}Ga are most often employed for oligopeptide PET tracers. It is important to note that ^{64}Cu and ^{86}Y occupy a favorablef middle ground with respect to radioactive half-life, allowing these radionuclides to be utilized advantageously in both antibody- and peptide-based based tracers.

The production of radiometals in high radionuclidic purity and specific activity is essential to the development of effective bioconjugates for PET imaging, and while an in-depth understanding of the nuclear reactions and purification chemistry behind their production may not be necessary for the biomedical use of these isotopes, a brief overview of the processes surely has merit. The production methods for radionuclides fall into three general categories: generator, cyclotron, and nuclear reactor (Fig. 2). Of the positron-emitting radiometals addressed in this perspective, ^{68}Ga is generator-produced, while ^{64}Cu, ^{86}Y, and ^{89}Zr are produced using a medical cyclotron.

^{68}Ga is produced *via* the electron capture decay of its parent radionuclide, ^{68}Ge. In the laboratory and clinic, ^{68}Ga can be produced using a compact, cost-effective, and convenient ^{68}Ge/^{68}Ga generator system, which is capable of providing ^{68}Ga for PET tracers for 1–2 years before being replaced.[69] The ^{68}Ga is eluted from the generator in 0.1 M HCl, providing a $^{68}GaCl_3$ starting material for radiolabeling.[70] Despite its convenience, the system does have some limitations, most notably high eluent volumes that often must be pH-adjusted prior to radiolabeling reactions, ^{68}Ge break-through from the generator, and metal-based impurities. However, a number of purification techniques have been developed to circumvent the problems presented by the trace impurities in the ^{68}Ga eluent.

^{86}Y is the first of the three cyclotron-produced radiometals to be addressed here. ^{86}Y is most often produced through the ^{86}Sr(*p*,*n*)^{86}Y reaction *via* bombardment of an isotopically enriched $^{86}SrCO_3$ or ^{86}SrO target with 8–15 MeV protons.[71–74] A range of purification methods have been employed, including combinations of precipitation, ion exchange chromatography, chromatography with a Sr-selective resin, and electrolysis.[75–77]

^{89}Zr has been produced *via* both the ^{89}Y(*p*,*n*)^{89}Zr and ^{89}Y(*d*,*2n*)^{89}Zr reactions. In the past, these methods have been used to successfully produce the radiometal using 13 MeV protons and 16 MeV deuterons, respectively, though both pathways have been complicated and limited by problematic purification protocols.[78–80] A significant improvement upon these methods was provided by another production strategy that yielded ^{89}Zr *via* the bombardment of ^{89}Y on a copper target with 14 MeV protons, oxidation of Zr^0 to Zr^{4+} with H_2O_2, and purification *via* anion exchange chromatography and subsequent sublimation steps.[81,82] In the last few years, these methods have been improved upon further through the use of an ^{89}Y thin-foil target (99% purity, 0.1 mm width), the optimization of bombardment conditions (15 MeV, 15 μA, 10° angle of incidence), and an improved solid phase hydroxamate resin purification to produce ^{89}Zr reliably and reproducibly in very high specific activity (470–1195 μCi/mmol) and radionuclidic purity (>99.99%).[83]

Finally, ^{64}Cu can be produced with either a nuclear reactor or a cyclotron *via* a variety of reaction pathways.[3] In a nuclear reactor, ^{64}Cu can be produced through the ^{63}Cu(*n*,*γ*)^{64}Cu and ^{64}Zn(*n*,*p*)^{64}Cu pathways. On a biomedical cyclotron, carrier-free ^{64}Cu can be produced using the ^{64}Ni(*p*,*n*)^{64}Cu and ^{64}Ni(*d*,*2n*)^{64}Cu reactions.[84–88] The former pathway has proven more successful and is currently used to provide ^{64}Cu to research laboratories throughout the United States. In this method, the ^{64}Cu is processed and purified *via* anion exchange chromatography to yield no carrier-added $^{64}Cu^{2+}$. The expense of the enriched ^{64}Ni target is a limitation of this production pathway, though a technique for the recycling of ^{64}Ni has ameliorated this issue somewhat. In the last few years, a number of groups have worked to develop methods for the production of ^{64}Cu using Zn targets through the ^{64}Zn(d, 2p)^{64}Cu,^{66}Zn(d,α)^{64}Cu, and ^{68}Zn(p,αn)^{64}Cu reactions.[89–92] These efforts have yielded some promising results but have failed to supplant the cyclotron-based ^{64}Ni(*p*,*n*)^{64}Cu pathway as the main route for ^{64}Cu production.

Radiometal chelation chemistry

With both the targeting vectors and radiometals in hand, the spotlight next falls on how to combine these two essential parts of the PET bioconjugate. Indeed, both the formation of a kinetically inert metal chelate and the stable covalent attachment of the chelator moiety to the biomolecule are essential to the creation of an effective radiopharmaceutical. To this end, a wide variety of metal-chelating molecules have been synthesized, studied, and, in many cases, made bifunctional to facilitate their conjugation to a biomolecular vector (Fig. 3 and 4, *vide infra*). Transition metal chelators fall into two broad classes: macrocylic chelators and acyclic chelators. Each has its own unique set of advantages: while macrocyclic chelators typically offer greater kinetic stability, acyclic chelators usually have

faster rates of metal binding. Generally, transition metal chelators offer at least four (and usually six or more) coordinating atoms, arrayed in a configuration that suits the preferred geometry of the oxidation state and d-orbital electron configuration of the metal in question. Yet simply having a generic chelator with well-organized and plentiful donor atoms is not enough; in every case, an appropriate chelator must be chosen to suit the selected radiometal (Table 3). Of course, however, some (*e.g.* DOTA) are more universally applicable than others (*e.g.* DiamSar). The most relevant oxidation states for the metals discussed here are Zr(IV), Ga(III), Y(III), and Cu(II); *in vivo*, only Cu(II) is at significant risk for reduction reactions. In terms of the commonly-employed 'hard-soft' system of classification, Zr(IV) is considered a very hard cation, with Y(III) and Ga(III) close behind on the spectrum. Cu(II), which is a borderline acid, straddles the hard/soft border and is thus easily the softest of the four.

Cu(II) has a rich chelation chemistry, capable of the formation of four-, five-, and six-coordinate complexes, with geometries ranging from square planar to trigonal bipyrimidal and octahedral.[3,30,32,36,42,93] Due to its position on the border between hard and soft metals, Cu(II) exhibits a great affinity for nitrogen donors, though it is also known to bind either harder oxygen or softer sulfur donors as well. Generally, a copper chelator will feature a mixture of uncharged nitrogen and anionic oxygen or sulfur donors in order to neutralize the charge of the dicationic metal. Alone in solution, the metal forms a five-coordinate aquo-complex with rapid water-exchange rates that translate into facile substitution reactions with other ligands.[94] Due to its $3d^9$ electronic structure, Cu(II) prefers a square planar coordination geometry. In consequence, both macrocyclic and acyclic tetradentate chelators have been developed for bioconjugation, including those with N_4 (*e.g.* cyclam), N_2O_2, and N_2S_2 (*e.g.* bis(aminothiolate)-based ligands) donor sets.[95,96] Due to the critical importance of kinetic stability, however, the complexation of Cu(II) with its maximum of six donor atoms has become more popular than the use of tetradentate chelators. To this end, both six-coordinate macro-cyclic and acyclic chelators have been employed with donor sets including N_2O_4 (*e.g.* EDTA), N_3O_3 (*e.g.* DTPA or NOTA), N_4O_2 (*e.g.* DOTA or CB-TE2A), and N_6 (*e.g.* SarAr, DiamSar, and AmBaSar).[54,97–101] Of these options, CB-TE2A and the SarAr family seem to be particularly promising, given their high kinetic and thermodynamic stability. The possibility of the reduction of Cu(II) to Cu(I) under physiological conditions with certain ligand sets must also be noted. In some cases (*e.g.* ^{64}Cu-ATSM), this reduction may be essential to the pharmacodynamics of the radiotracer; however, in most situations, it is an extremely undesirable behavior that compromises the integrity of the radiopharmaceutical.[24]

Smaller and harder than Cu^{2+}, the Ga^{3+} cation typically binds ligands containing multiple anionic oxygen donors and adopts a coordination number of six, though complexes with four or five donor atoms are also known.[36,38,44,102,103] Aqueous pH is particularly important in Ga^{3+} chelation chemistry: the low pK_a of the $Ga(H_2O)_6^{3+}$ complex results in low solubility at physiological pH, while under basic conditions the affinity of the metal for hydroxide anions can result in its dissociation from chelators to form gallium hydroxide species. Tetradentate chelators with NO_3, NS_3, and N_2S_2 donor sets have been used.[104–106] These polydentate ligands often combine with one or two water molecules or halides to place the metal in a distorted octahedral or distorted square pyramidal geometry; however, in some cases, the Ga^{3+} can adopt a simple four-coordinate distorted tetrahedral geometry. Acyclic and macrocylic hexadentate chelators are more common for Ga^{3+}, including those with $N_2O_2S_2$ (*e.g.* bis(aminothiolate)-based ligands), N_2O_4 (HBED), N_3O_3 (NOTA), N_3S_3 (TACN-TM), N_4O_2 (DOTA), and O_6 (DFO) donor sets.[102,107–110] Complexes bearing these ligands almost always adopt a distorted octahedral geometry. Amongst these, DOTA is easily the most commonly employed in bioconjugates. However, the ligand has two drawbacks that limit its suitability for $^{68}Ga^{3+}$.[111] A central cavity that is too large for the

cation limits the stability of the complex, and sluggish complexation kinetics require reaction times and temperatures that are less than ideally compatible with the short half-life of ^{68}Ga and the stability of some biomolecular constructs, respectively. In contrast, TACN-TM and HBED- and NOTA-based ligands are particularly promising chelation systems for ^{68}Ga due to their high thermodynamic and kinetic stability.[103,112,113]

The chemistry of Y(III) provides a significant change of pace from the previous two metals. Much larger than the three other common PET radiometals, the closed-shell, hard Y^{3+} cation often reaches coordination numbers of eight or nine. Donor sets of N_2O_4 (EDTA), N_3O_3 (NOTAM), N_3O_5 (DTPA), N_4O_4 (DOTA), and N_4O_2 (TETA) have all been used to chelate the metal, with water molecules or other exogenous ligands filling the remaining coordination sites.[114–117] The DOTA and DTPA ligands, however, form much more stable complexes with the metal than TETA and EDTA, indicating better chelator-metal matches in the former cases. The higher coordination numbers also result in more exotic geometries: the DTPA complex adopts a monocapped square antiprism structure, the EDTA complex assumes a distorted dodecahedron geometry, and the DOTA complex results in a square antiprism structure. To date, DOTA- and DTPA-based chelators have been used in the vast majority of ^{86}Y bioconjugate strategies, though future studies will no doubt expand the range of chelating moieties employed in these tracers.[118–120]

^{89}Zr is easily the most recent addition to the family of common PET radiometals, and the relative scarcity of aqueous chelation chemistry studies reflects this fact. The highly cationic Zr^{4+} center exhibits a strong preference for ligands bearing multiple anionic oxygens and can accommodate up to nine coordinating atoms. The metal makes eight-coordinate, dodecahedral complexes with DTPA (N_3O_5), EDTA (N_2O_4 with two additional water ligands), and DOTA (N_4O_4, though the evidence here is less clear).[121,122] However, the overwhelming majority of ^{89}Zr-bioconjugates employ DFO as the chelating ligand.[123,124] No solid state or NMR structural studies are available, though DFT calculations suggest that seven- or eight-coordinate species involving one or two water molecules in addition to the ligand's six oxygen donors are most likely.[125] Given the considerable potential of ^{89}Zr as a PET radiometal, the continued development of novel high-stability chelating systems is needed.

Conjugation strategies

The final piece of the anatomy of a radiometal PET bioconjugate is the covalent attachment of the chelator to the biomolecule. This link must be stable under physiological conditions and must not significantly compromise the binding strength and specificity of the biomolecule. Three bond-types comprise the overwhelming majority of chelator-biomolecule attachments: peptide, thiourea, and thioether bonds (Fig. 5). The first of these three attachments is formed through the reaction of an activated carboxylic acid and a primary amine, the second *via* an isothiocyanate and an amine, and the third *via* a thiol and a maleimide. These are not, however, the only options for the conjugation reaction; the reactions of vinylsulfones with thiols, bromoacetamides with amines, and bromoacetamides with thiols have also been employed in more unique cases. Further still, and more recently, the set of bioorthogonal cycloaddition reactions, broadly termed “click chemistry” reactions, have also been applied to chelator conjugations (*vide infra*).

To facilitate the formation of these covalent links, bifunctional chelators are often employed. Bifunctional chelators are molecules bearing both metal-binding moieties and either reactive bond-making functionalities or pendant linker arms (Fig. 3 and 4). Given the preponderance of available primary amines and free thiols on many biomolecules, the corresponding activated ester, isothiocyanate, and maleimide groups are usually incorporated into the bifunctional chelator. These molecules can be synthesized and isolated from known

chelators (*e.g.* DOTA-NHS from DOTA), designed and synthesized *de novo* as bifunctional chelators (*e.g. p*-SCN-Bn-DOTA), or generated *in situ* prior to or during the conjugation reaction (*e.g.* DOTA(tBu)$_3$-NHS from DOTA(tBu)$_3$). In some cases, the modification to a chelator that confers bifunctionality is made at a point that otherwise may have been a metal donor site, for example the addition of an activated ester to a carboxylate arm in DOTA-NHS; in other situations, for example *p*-SCN-Bn-DOTA, a bifunctional linker is built into the backbone of the chelator so as to minimize any interference with the molecule's ability to bind to metal ions.

Both the number of chelates per biomolecule and the control over their placement can vary widely. The smaller size, well-established protecting group chemistry, and highly controlled and automated synthesis of peptide and nucleic acid vectors often allow for only a single chelator moiety, positioned at one terminus of the oligomer. In contrast, the method by which bifunctional chelators are typically conjugated to antibodies, *i.e.* the simple incubation of a given number of equivalents of bifunctional chelator with a solution of antibody, results in both a variable number of chelating moieties per antibody and their indeterminate placement on the macromolecule. The number of chelators per antibody can be determined fairly easily using isotopic dilution methods and can be controlled simply by altering the molar ratio of the bifunctional chelator in the conjugation reaction. Generally, more chelators per antibody is preferable, because higher specific activities can be attained. The control and knowledge of chelator placement, however, is harder to come by; the apprehension here, of course, is that the presence of a chelator in the binding region of the antibody can negatively effect its ability to bind to the antigen. Therefore, the goal in antibody conjugation is simple: attach as many chelators per antibody as possible, without compromising the immunoreactivty of the biomolecule.

Significantly, the conjugation of the chelator is almost always performed prior to radiometallation. Thus, the final step in the construction of a PET radiometal bioconjugate is the radiolabeling of the biomolecule-linker-chelator construct. The goal of this final step is the incorporation of as much activity as possible, as quickly as possible, without damaging the biomolecule. Therefore, temperature and pH conditions that favor rapid metallation reactions must be balanced against the concern for the integrity of the biomolecule. For example, while metallating a DOTA-conjugated antibody with ^{64}Cu may proceed most quickly and efficiently at 90 °C, such high temperatures risk denaturing the antibody, and lower temperatures should be employed as a result.

In the preceding pages, it has become clear that the imaging scientist has many choices to make and factors to consider in the development and construction of a radiometal-based PET bioconjugate. In the final section of this perspective, we will provide a practical overview of the design and synthesis strategies used for PET bioconjugates currently described in the literature.

The construction of ^{68}Ga bioconjugates

The short half-life and facile production of ^{68}Ga have made it one of the radionuclides of choice for peptide-based PET bioconjugates.[126] Tracers have been developed to target a wide array of cancer biomarkers, including epidermal growth factor receptor (EGFR), gastrin releasing peptide receptor (GRPR), integrin $\alpha_v\beta_3$, and melanocortin-1 receptor (MC1-R).[127–130] However, the ^{68}Ga peptide bioconjugates that have had the greatest impact in the clinic are without question the family of ^{68}Ga-somatostatin analogues (SST).[131–134] SST-receptors (SSTR) are over-expressed in neuroendorcrine tumors, prostate carcinomas, breast carcinomas, lymphomas, and small-cell lung cancers, among others, and ^{68}Ga-somatostatin analogues, particularly ^{68}Ga-DOTATOC, have been used to great effect in the imaging of these malignancies (Fig. 6).[135]

A wide variety of chelators, conjugation strategies, and metallation procedures have been employed in the synthesis of ^{68}Ga-labeled peptides (see Table 4 for experimental details and references). DOTA and NOTA-conjugated peptides are most common by a wide margin, though HBED and DFO have also been used. Given the solid-phase synthesis of many peptides, the conjugation of the chelator to the peptide is often performed while the peptide is still attached to a solid resin support. This can be achieved *via* the manual manipulation of the peptide-coated resin and subsequent incubation with a bifunctional chelator, or using an automated peptide synthesizer. In the latter scenario, a pre-prepared bifunctional chelator is not needed; rather, a monoreactive precursor is added to the automated synthesizer and is coupled to the growing peptide chain *via* an activated, bifunctional intermediate. Despite the preponderance of solid-phase methods, a number of *in situ* conjugations have also been reported using bifunctional chelators such as DOTA-NHS, HBED-CC-NHS, *p*-SCN-Bn-NOTA, and NH_2-Bn-NOTA. Generally, peptide and isothiocyanate-based conjugations are performed at a slightly basic pH (8–9.5), due to the participation of a deprotonated primary amine in the bond-forming reactions. Further still, the peptide-chelator conjugates are almost always purified *via* RPHPLC or C_{18} cartridge prior to radiolabeling.

The metallation procedures for the peptide-chelator constructs follow the same general course, though the experimental details can vary considerably. The most common buffers for the metallation reaction are NaOAc, HEPES, NaH_2PO_4/Na_2HPO_4, and Na_2CO_3/$NaHCO_3$, and these are used in concentrations ranging from 0.1 M to 0.5 M. The pH for the reaction depends on the chelator: 5–6 for NOTA-based chelators, 3.8–5.5 for DOTA-based chelators, 4–5 for HBED, and 4–5 for DFO. Reaction times and temperatures likewise vary depending on the chelator employed, ranging from 5 min at room temperature for DFO to 25 min at 95 °C and 20 min at 100 °C for DOTA. Often, the radiolabeling reaction is quenched by the addition of free chelator to scavenge excess unreacted radiometal. Finally, the purification of the resultant radiolabeled peptides is most often achieved using C18 cartridges (*e.g.* Waters Sep-Pak^{TM}), RP-HPLC, or size exclusion chromatography.

^{68}Ga has also been used for the labeling of antibody fragments and affibody molecules, though far fewer examples exist than for ^{68}Ga-peptides (see Table 5 for experimental details and references). In these cases, HBED, DOTA, and DTPA have been employed as the chelators of choice. The conjugation reactions are usually performed *via* the incubation of a solution of antibody fragment with a bifunctional chelator, such as DOTA-NHS or HBEDCC-TFP; however, in the case of one affibody construct, solid phase peptide synthesis and a monoreactive chelator precursor are used as described above for the peptide-based conjugates. Again, all of the macromolecules are purified subsequent to conjugation in order to remove excess chelator. Despite the relatively few examples, the metallation reactions are performed using an array of buffer types (HEPES, phosphate, and NH_4OAc) and concentrations (0.1 M to 1.25 M). The time, temperature, and pH of the metallation reactions are all dependent on the identity of the chelator, though in a few cases, these conditions are not noted in the literature. After a suitable incubation, the radiolabeling reaction is often quenched with the addition of free chelator, and in all cases, the resultant radiometallated conjugate is purified with size exclusion chromatography. It thus becomes clear that the labeling of antibody fragments does not yet have standardized methodologies, which is a limitation that will be resolved as more examples of these extremely promising radiotracers come to light.

Finally, a small number of oligonucleotide-based ^{68}Ga-labeled bioconjugates have also been developed (see Table 6 for experimental details and references).[136–138] 2′-Deoxyphosphodiester (PO), 2′-deoxyphosphorthioate (PS), 2′-*O*-methyl phosphodiester (OMe), and locked nucleic acid (LNA) oligonucleotides have been synthesized and radiolabeled for gene expression imaging. In all cases, DOTA has been used as the chelator

for ^{68}Ga and is incorporated into the oligonucleotide using a DOTA-SNHS bifunctional chelate. Metallations have been performed in either NaOAc or HEPES buffer at pH 4.5–5.5, using short incubations at 90–100 °C (in some cases, microwave-assisted). Finally, the completed, radiolabeled oligonucleotides are typically purified with reverse-phase C_4 or C_{18} cartridges (*e.g.* Waters Sep-Pak^{TM}).

The construction of ^{64}Cu bioconjugates

Given its intermediate half-life, favorable decay properties, relative accessibility, and well-established chelation chemistry, ^{64}Cu has become a versatile and widely utilized radiometal for bioconjugate tracers. A variety of ^{64}Cu-peptides have been developed, targeting biomarkers including SSTR, integrin $\alpha_v\beta_3$, GRPR, MC1-R, integrin $\alpha_4\beta_1$, formyl peptide receptor (FPR), natriuretic peptide receptor (NPR), and vascular endothelial growth factor receptor (VEGFR), among many others (Fig. 7, see Table 7 for experimental details and references). The chelators employed in these conjugates are almost as diverse as the peptides themselves, with DOTA and CB-TE2A leading the way, but with TETA, NOTA, BPM-TACN, and DiamSar also used in some agents. As in the ^{68}Ga peptides, both solid- and solution-phase chelator conjugation strategies have been used. For those involving bifunctional chelators, peptide and isothiocyanate-based conjugations are typically performed at slightly basic pH (8–9.5), because these reactions require a deprotonated primary amine to proceed. Also like the ^{68}Ga cases, the post-conjugation purification of the peptide-chelator construct by RP-HPLC or C_{18} cartridge is a common practice. The buffers most often chosen for radiometallations are NH_4OAc and NaOAc, typically utilized at concentrations ranging from 0.1 M to 0.5 M. However, incubation time, temperature, and pH vary according to the chelator. For example, the radiolabeling of DOTA-based conjugates is typically performed at pH 5–6.5 with 30–60 min incubations at temperatures ranging from room temperature to 95 °C. In contrast, the metallation of DiamSar-based conjugates can be performed at pH 8.0 with a 60 min incubation at room temperature. In many cases, unreacted ^{64}Cu is scavenged after radiolabeling with free chelator (*e.g.* EDTA or DTPA), and after the successful radiometallation reaction, the overwhelming majority of the ^{64}Cu-peptide conjugates are purified using RP-HPLC.

The 12.7 h half-life of ^{64}Cu has allowed it to be utilized in antibody-based conjugates as well as those derived from peptides (see Table 8 for experimental details and references). Indeed, ^{64}Cu-labeled antibody radiotracers have been developed against an array of biomarker antigens, for example human epidermal growth factor receptor 2 (HER2), prostate specific membrane antigen (PSMA), epidermal growth factor receptor (EGFR), and carcinoembryonic antigen (CEA). As with the ^{64}Cu-peptides, a number of chelators have been used, including DOTA, CPTA, DO3A, TETA, and SarAr. The conjugation strategies for antibodies rely almost exclusively on incubation with bifunctional chelators, either generated *in situ* or synthesized and isolated (or purchased) beforehand. As is now clearly becoming a trend, the antibody-chelator constructs are almost always purified after conjugation by size exclusion chromatography or centrifugation with a high molecular weight filter membrane. The metallation procedures closely resemble those used for ^{64}Cu-peptides: the most common buffers are NaOAc, NH_4OAc, and NH_4-citrate at concentrations of 0.1–0.25 M. The incubation time, temperature, and pH vary according to chelator; however, the incubation temperatures seldom rise above 43 °C due to concerns over antibody stability. Again, in many cases, unreacted ^{64}Cu is scavenged after radiolabeling with free chelator (*e.g.* EDTA or DTPA). Finally, the radiometallated antibody bioconjugates are typically purified *via* size exclusion chromatography (*e.g.* HPLC, FPLC, or GE Life Sciences PD-10 columns) or centrifugal column filtration (*e.g.* Amicon Ultra-4 30,000 MWCO centrifugal filtration units).

A small number of peptide nucleic acid (PNA) and hybrid PNA-oligopeptide ^{64}Cu-labeled conjugates have also been created for mRNA-targeted imaging (see Table 6 for experimental details and references). These conjugates have employed either DOTA or $SBTG_2DAP$ as the chelating moieties, with solid-phase Fmoc synthesis techniques analogous to those for peptides used to incorporate the chelators into the oligomers. Radiolabeling reactions have been performed in either NH_4OAc or NH_4-citrate buffer (pH 5.5–6.0), with incubations of 15–120 min at temperatures ranging from 60 to 90 °C.

The construction of ^{86}Y bioconjugates

The intermediate half-life, well-studied chelation chemistry, and presence of a radiotherapeutic isotopologue in ^{90}Yall make ^{86}Ya promising PET radiometal. However, decay properties that result in a lower image quality than ^{89}Zr, ^{64}Cu, and ^{68}Ga and difficulties in its production and purification have limited the development of ^{86}Y bioconjugates. Nevertheless, a number of ^{86}Y-based antibody, peptide, and oligonucleotide PET radiopharmaceuticals have been successfully synthesized and evaluated (see Table 9 for experimental details and references). For example, radiolabeled antibodies against EGFR, human epidermal growth factor 1 (HER1), Lewis Y antigen, and mindin/RG1 have been developed (Fig. 8). All of these conjugates have been synthesized *via* incubation of antibody with the CHX-A″-DTPA bifunctional chelator under basic buffer conditions, followed by purification steps to separate the bioconjugate from unreacted chelator. Radiolabeling reactions are typically performed in NH_4OAc buffer (0.1–3.0 M, pH 5–6) with incubations of 30–60 min at room temperature, followed by quenching with free chelator (*e.g.* DTPA or EDTA). The resultant completed bioconjugates are purified *via* size exclusion chromatography (*e.g.* HPLC, FPLC, or PD-10 columns) to remove any unbound ^{86}Y.

In addition to the antibody-based tracers, a variety peptide-based agents have been synthesized, including agents targeting MC1-R, SSTR, and GRPR. In these conjugates, CHX-A″-DTPA and DOTA have been the predominant chelators employed, with both solid-phase synthesis and bifunctional chelator conjugation routes utilized. Not surprisingly, the radiometallation conditions are dependent upon the chelator, though NaOAc and NH_4OAc buffers and pH values of 5–7 are most common. To complete the synthesis, the radiometallated peptide conjugates are almost all purified using RP-HPLC with C_{18} or C_4 columns.

An isolated few ^{86}Y-labeled RNA-based conjugates have also been synthesized for mRNA targeted imaging (see Table 6 for experimental details and references). These conjugates all utilize DOTA for ^{86}Y chelation, and the chelator is incorporated into the oligomer *via* reaction with *p*-SCN-Bn-DOTA. Radiolabeling is accomplished *via* incubation of the chelator-RNA construct with ^{86}Y in NH_4OAc (0.5 M, pH 7.0) for 30–60 min at 90 °C. Unfortunately, however, only two publications on ^{86}Y-labeled oligonucleotide radiotracers currently exist in the literature, so more general procedures and guidelines cannot be presented here.

The construction of ^{89}Zr bioconjugates

Due to its long half-life, ^{89}Zr has been used almost exclusively in the formation of antibody bioconjugates. Yet despite this narrow range of application, a wide array of antibody-based radiopharmaceuticals have been developed, including those targeting EGFR, VEGFR, carbonic anhydrase IX (CAIX), HER2, PSMA, and B-lymphocyte antigen CD20 (CD20) (Fig. 9, see Table 10 for experimental details and references). Interestingly, one chelator, DFO, has been employed in the overwhelming majority of these bioconjugates. Two routes have dominated the reported chelator conjugations: (1) the peptide coupling of a TFP ester

of an Fe^{III}(DFO) complex to the antibody of choice, followed by the removal of the Fe^{3+} cation and (2) the incubation of the antibody with a bifunctional DFO-SCN chelator. More recently, however, promising site-specific conjugation routes using maleimide- and halide-modified DFO have been reported. Regardless of the route, the resultant conjugate is typically purified *via* size exclusion chromatography to remove unbound chelate and subsequently metallated with ^{89}Zr at pH 6.7–8.5 in buffer (HEPES and/or carbonate), with incubations of 30–120 min at room temperature. In all cases, the resultant radiolabeled bioconjugate is purified *via* size exclusion chromatography (most often GE Life Sciences PD-10 columns).

Frontiers in bioconjugate development

Both in the laboratory and in the clinic, the field of radiometallated PET bioconjugates is progressing at an exciting rate. Indeed, researchers are currently pushing back the frontiers for all of the components of the bioconjugate anatomy. To be sure, the arena with the most limited prospects is the choice of radiometal, however, efforts do exist to expand the family of PET radiometals used for bioconjugates to include new possibilities, such as ^{45}Ti and ^{74}As.[39,40,61,68] The development of new biomolecular vectors is a particularly fertile area, with the discovery of new cancer biomarkers and advances in protein engineering fueling this growth. Interestingly, an increasing number of vectors are being studied, which target not specific cell-surface proteins or gene products but rather characteristics of the tumor microenvironment.[56]

Yet most relevant to the discussion at hand is the forefront of research on chelation, metallation, and conjugation strategies. New chelating architectures and bifunctional chelators are being designed and synthesized at a tremendous rate, often out-stripping the pace of the development of new bioconju-gates themselves.[30–32,139] The advent of rapid, bioorthogonal, and chemoselective ‘click chemistry’ reactions represents a particularly exciting new approach to chelator conjugation.[140–144] While the exact definition of click chemistry can vary, the most common example is the copper-catalyzed 1,3-dipolar Huisgen cycloaddition between an azide and an alkyne. The reaction is rapid, high-yielding, clean, and chemoselective and has already been extensively employed in ^{18}F-based PET radiotracers.[142,145,146] However, the application of click chemistry to radiometal probes has lagged behind somewhat, perhaps due to concern over Cu(I) contamination from the cycloaddition catalyst. Nonetheless, a small number of ‘clickable’ bifunctional chelators and their resultant bioconjugates have begun to appear in the literature, including DOTA and CB-TE2A examples.[147,148] Further, the development of new click reactions that do not require a copper catalyst, including [3+2] cycloadditions between azides and strained alkynes,[149,150] inverse electron demand Diels–Alder cycloadditions between tetrazines and strained dienophiles,[151,152] and azaelectrocyclizations,[153] have begun to capture the interest of radiochemists and will surely soon occupy an important place in the synthesis of novel bioconjugates. Finally, the most exciting developments in radiolabelling lie in the full automation of bioconjugate radiometallation and, perhaps ultimately, chelator conjugation as well.[154] Such developments will increase standardization and reproducibility while concomitantly decreasing radiation dose rates to researchers.

Conclusions

In the preceding pages, we have detailed the synthesis of radiotracers using four different radiometals, tens of biomolecular vectors, over thirty chelating scaffolds, and a myriad of different conjugation and metallation strategies. This diversity is the hallmark of an important and rapidly growing field, one that is increasingly attracting the attention of scientists from a wide variety of other specialities. Indeed, during the writing of this perspective, three new bioconjugates were published that required inclusion; between

submission and publication, even more will likely appear in the literature. This influx of new interest is a boon to the molecular imaging community, bringing with it new expertise and perspectives. The rapid pace of development in this area, however, may inadvertently act as an obstacle to new researchers, simply due to the sheer number of conjugation and metallation protocols, which can vary by as much as the identity of a radiometal or by as a little as a tenth of a pH unit. Therefore, we believe it is extremely important not only to encourage the development of diverse strategies for the synthesis of PET bioconjugates but also to make these experimental methods widely accessible and straightforward to the field as a whole. Our hope is that this perspective will aid in this effort.

Acknowledgments

First and foremost, the authors would like to thank all of those researchers whose work has contributed to the imaging agents discussed in these pages. Compiling this perspective has made us ever more aware of the intellectual vibrancy of this field and the scientists within it. More specifically, we would like to thank Dr Jason Holland and Dr NagaVaraKishore Pillarsetty for helpful discussions. We would also like to thank the NIH for their generous funding [NIH R01 CA138468 (JSL) and NIH F32 CA144138 (BMZ)].

References

1. Rudin M, Weissleder R. Nat Rev Drug Discovery. 2003; 2:123–131.
2. Gillies RJ. J Cell Biochem. 2002; 87(S39):231–238.
3. Smith SV. J Inorg Biochem. 2004; 98:1874–1901. [PubMed: 15522415]
4. Blower P. Dalton Trans. 2006:1705–1711. [PubMed: 16568178]
5. Mettler, JFA.; Guiberteau, MJ. Essentials of Nuclear Medicine Image. 5. 2007.
6. Dilworth JR, Parrott SJ. Chem Soc Rev. 1998; 27:43–55.
7. Verel I, Visser GWM, van Dongen GA. J Nucl Med. 2005; 46S1:164S–171S. [PubMed: 15653665]
8. Mahmood A, Jones AG. Handbook of Radiopharmaceuticals. 2003:323–362.
9. Liuand S, Edwards DS. Chem Rev. 1999; 99:2235–2268. [PubMed: 11749481]
10. Brownell GL, Sweet WH. Nucleonics. 1953; 11:40–45.
11. Sweet WH. N Engl J Med. 1951; 245:875–878. [PubMed: 14882442]
12. Sweet WH, Brownell GL. Journal of the American Medical Association. 1955; 157:1183–1188. [PubMed: 14353655]
13. Wrenn FRJ, Good ML, Handler P. Science. 1951; 113:525–527. [PubMed: 14828392]
14. Bagnall HJ, Benda P, Brownell GL, Sweet WH. J Neurosurg. 1958; 15:411–426. [PubMed: 13564268]
15. Tang Y, Scollard D, Chen P, Wang J, Holloway C, Reilly RM. Nucl Med Commun. 2005; 26:427–432. [PubMed: 15838425]
16. Knight LC. Handbook of Radiopharmaceuticals. 2003:643–684.
17. Anderson CJ, Connett JM, Schwarz SW, Rocque PA, Guo LW, Philpott GW, Zinn KR, Meares CF, Welch MJ. J Nucl Med. 1992; 33:1685–1691. [PubMed: 1517844]
18. Schrama D, Reisfeld RA, Becker JC. Nat Rev Drug Discovery. 2006; 5:147–159.
19. Zalutsky MR, Lewis JS. Handbook of Radiopharmaceuticals. 2003:685–714.
20. Ruangma A, Bai B, Lewis JS, Sun X, Welch MJ, Leahy R, Laforest R. Nucl Med Biol. 2006; 33:217–226. [PubMed: 16546676]
21. Beer AJ, Grosu AL, Carlsen J, Kolk A, Sarbia M, Stangier I, Watzlowik P, Wester HJ, Haubner R, Schwaiger M. Clin Cancer Res. 2007; 13:6610–6616. [PubMed: 18006761]
22. Divgi CR, Pandit-Taskar N, Jungbluth AA, Reuter VE, Gönen M, Ruan S, Pierre C, Nagel A, Pryma DA, Humm J, Larson SM, Old LJ, Russo P. Lancet Oncol. 2007; 8:304–310. [PubMed: 17395103]
23. Wong TZ, Lacy JL, Petry NA, Hawk TC, Sporn TA, Dewhirst MW, Vlahovic G. AJR, Am J Roentgenol. 2008; 190:427–432. [PubMed: 18212229]

24. Lewis JS, McCarthy DW, McCarthy TJ, Fujibayashi Y, Welch MJ. J Nucl Med. 1999; 40:177–183. [PubMed: 9935074]
25. Vavere AL, Lewis JS. Dalton Trans. 2007:4893–4902. [PubMed: 17992274]
26. Dehdashti F, Grigsby PW, Lewis JS, Laforest R, Siegel BA, Welch M. J Nucl Med. 2008; 49:201–205. [PubMed: 18199612]
27. Lewis JS, Laforest R, Dehdashti F, Grigsby PW, Welch MJ, Siegel BA. J Nucl Med. 2008; 49:1177–1182. [PubMed: 18552145]
28. Holland JP, Lewis JS, Dehdashti F. Q J Nucl Med Mol Imag. 2009; 53:193–200.
29. Viola-Villegas N, Doyle RP. Coord Chem Rev. 2009; 253:1906–1925.
30. Wadas TJ, Wong EH, Weisman GR, Anderson CJ. Chem Rev. 2010; 110:2858–2902. [PubMed: 20415480]
31. Mewis RE, Archibald SJ. Coord Chem Rev. 2010; 254:1686–1712.
32. Wadas TJ, Wong EH, Weisman GR, Anderson CJ. Curr Pharm Des. 2007; 13:3–16. [PubMed: 17266585]
33. ISI Web of Knowledge v.4.10. [Accessed October 26, 2010]
34. Boswell CA, Brechbiel MW. Nucl Med Biol. 2007; 34:757–778. [PubMed: 17921028]
35. Dunphy MPS, Lewis JS. J Nucl Med. 2009; 50:106S–121S. [PubMed: 19380404]
36. Liu S. Chem Soc Rev. 2004; 33:445–461. [PubMed: 15354226]
37. van Dongen GAMS, Visser GWM, Lub-de Hooge MN, de Vries EG, Perk LR. Oncologist. 2007; 12:1379–1389. [PubMed: 18165614]
38. Anderson CJ, Welch MJ. Chem Rev. 1999; 99:2219–2234. [PubMed: 11749480]
39. Lewis JS, Singh RK, Welch Michael J. Long Lived and Unconventional PET Radionuclides. 2009
40. Holland JP, Williamson MJ, Lewis JS. Mol Imaging. 2010; 9:1–20. [PubMed: 20128994]
41. Nayak TK, Brechbiel MW. Bioconjugate Chem. 2009; 20:825–841.
42. Shokeen M, Anderson CJ. Acc Chem Res. 2009; 42:832–841. [PubMed: 19530674]
43. Anderson CJ, Ferdani R. Cancer Biother Radiopharm. 2009; 24:379–393. [PubMed: 19694573]
44. Al-Nahhas A, Win Z, Szyszko T, Singh A, Nanni C, Fanti S, Rubello D. Anticancer Res. 2007; 27:4087–4094. [PubMed: 18225576]
45. Brechbiel MW. Q J Nucl Med Mol Imag. 2008; 52:166–173.
46. Goldenberg DM, Rossi EA, Sharkey RM, McBride WJ, Chang CH. J Nucl Med. 2008; 49:158–163. [PubMed: 18077530]
47. Schoffelen R, Sharkey RM, Goldenberg DM, Franssen G, McBride WJ, Rossi EA, Chang CH, Laverman P, Disselhorst JA, Eek A, Van Der Graaf WTA, Oyen WJG, Boerman OC. Mol Cancer Ther. 2010; 9:1019–1027. [PubMed: 20354120]
48. Cai WB, Chen XY. J Nucl Med. 2008; 49:113S–128S. [PubMed: 18523069]
49. Cheon J, Lee JH. Acc Chem Res. 2008; 41:1630–1640. [PubMed: 18698851]
50. Eiblmaier M, Andrews R, Laforest R, Rogers BE, Anderson CJ. J Nucl Med. 2007; 48:1390–1396. [PubMed: 17631550]
51. Cai WB, Wu Y, Chen K, Cao QZ, Tice DA, Chen XY. Cancer Res. 2006; 66:9673–9681. [PubMed: 17018625]
52. Biddlecombe GB, Rogers BE, de Visser M, Parry JJ, de Jong M, Erion JL, Lewis JS. Bioconjugate Chem. 2007; 18:724–730.
53. Cai WB, Chen K, He LN, Cao QH, Koong A, Chen XY. Eur J Nucl Med Mol Imaging. 2007; 34:850–858. [PubMed: 17262214]
54. Voss SD, Smith SV, DiBartolo N, McLntos LJ, Cyr EM, Bonab AA, Dearling JLJ, Carter EA, Fischman AJ, Treves ST, Gillies SD, Sargeson AM, Huston JS, Packard AB. Proc Natl Acad Sci USA. 2007; 104:17489–17493. [PubMed: 17954911]
55. Tian XB, Winter R, Aruva MR, Zhang KJ, Cardi CA, Thakur ML, Wickstrom E. Clin Cancer Res. 2005; 11:9130S–9130S.
56. Vavere AL, Biddlecombe GB, Spees WM, Garbow JR, Wijesinghe D, Andreev OA, Engelman DM, Reshetnyak YK, Lewis JS. Cancer Res. 2009; 69:4510–4516. [PubMed: 19417132]

57. Dehdashti F, Mintun MA, Lewis JS, Bradley J, Govindan R, Laforest R, Welch MJ, Siegel BA. Eur J Nucl Med Mol Imaging. 2003; 30:844–850. [PubMed: 12692685]
58. Bigott HM, Parent E, Luyt LG, Katzenellenbogen JA, Welch MJ. Bioconjugate Chem. 2005; 16:255–264.
59. Buck A, Nguyen N, Burger C, Ziegler S, Frey L, Weigand G, Erhardt W, Senekowitsch-Schmidtke R, Pellikka R, Blauenstein P, Locher JT, Schwaiger M. Eur J Nucl Med Mol Imaging. 1996; 23:1619–1627.
60. Haynes NG, Lacy JL, Nayak N, Martin CS, Dai D, Mathias CJ, Green MA. J Nucl Med. 2000; 41:309–314. [PubMed: 10688116]
61. Vavere AL, Welch MJ. J Nucl Med. 2005; 46:683–690. [PubMed: 15809492]
62. Bruehlmeier M, Leenders KL, Vontobel P, Calonder C, Antonini A, Weindl A. J Nucl Med. 2000; 41:781–787. [PubMed: 10809192]
63. Srivastava SC, Kolsky KL, Mease RC, Joshi V, Meinken GE, Pyatt B, Wolf AP, Schlyder DJ, Levy AV, Fowler JS. J Labelled Comp Rad. 1994; 35:389–391.
64. Wallberg H, Ahlgren S, Widstrom C, Orlova A. Mol Imaging Biol. 2010; 12:54–62. [PubMed: 19557480]
65. Ugur O, Kothari PJ, Finn RD, Zanzonico P, Ruan S, Guenther I, Maecke HR, Larson SM. Nucl Med Biol. 2002; 29:147–157. [PubMed: 11823119]
66. Lubberink M, Tolmachev V, Widstrom C, Bruskin A, Lundqvist H, Westlin JE. J Nucl Med. 2002; 43:1391–1397. [PubMed: 12368379]
67. Jennewein M, Hermanne A, Mason RP, Thorpe PE, Rosch F. Nucl Instrum Methods Phys Res, Sect A. 2006; 569:512–517.
68. Jennewein M, Lewis MA, Zhao D, Tsyganov E, Slavine N, He J, Watkins L, Kodibagkar VD, O'Kelly S, Kulkarni P, Antich PP, Hermanne A, Rosch F, Mason RP, Thorpe PE. Clin Cancer Res. 2008; 14:1377–1385. [PubMed: 18316558]
69. Ehrhardt GJ, Welch MJ. J Nucl Med. 1978; 19:925–929. [PubMed: 98618]
70. Zhernosekov KP, Filosofov DV, Baum RP, Aschoff P, Bihl H, Razbash AA, Jahn M, Jennewein M, Rosch F. J Nucl Med. 2007; 48:1741–1748. [PubMed: 17873136]
71. Sadeghi M, Aboudzadeh M, Zali A, Mirzaii M, Bolourinovin F. Appl Radiat Isot. 2009; 67:7–10. [PubMed: 18930657]
72. Sadeghi M, Aboudzadeh M, Zali A, Zeinali B. Appl Radiat Isot. 2009; 67:1392–1396. [PubMed: 19285420]
73. Sadeghi M, Zali A, Aboudzadeh M, Sarabadani P, Aslani G, Majdabadi A. Appl Radiat Isot. 2009; 67:2029–2032. [PubMed: 19110437]
74. Park LS, Szajek LP, Wong KJ, Plascjak PS, Garmestani K, Googins S, Eckelman WC, Carrasquillo JA, Paik CH. Nucl Med Biol. 2004; 31:297–301. [PubMed: 15013497]
75. Avila-Rodriguez MA, Nye JA, Nickles RJ. Appl Radiat Isot. 2008; 66:9–13. [PubMed: 17869530]
76. Lukic D, Tamburella C, Buchegger F, Beyer GJ, Comor JJ, Seimbille Y. Appl Radiat Isot. 2009; 67:523–529. [PubMed: 19181533]
77. Yoo J, Tang L, Perkins TA, Rowland DJ, Laforest R, Lewis JS, Welch MJ. Nucl Med Biol. 2005; 32:891–897. [PubMed: 16253815]
78. DeJesus OT, Nickles RJ. Int J Radiat Appl Instrum, Part A. 1990; 41:789–790.
79. Zweit J, Downey S, Sharma HL. Int J Radiat Appl Instrum, Part A. 1991; 42:199–201.
80. Link JM, Krohn KA, Eary JF, Kishore R, Lewellen TK, Johnson MW, Badger CC, Richter KY, Nelp WB. J Labelled Comp Rad. 1986; 23:1297–1298.
81. Verel I, Visser GWM, Boellaard R, Stigter-van Walsum M, Snow GB, van Dongen G. J Nucl Med. 2003; 44:1271–1281. [PubMed: 12902418]
82. Meijs WE, Herscheid JDM, Haisma HJ, Wijbrandts R, van Langevelde F, van Leuffen PJ, Mooy R, Pinedo HM. Appl Radiat Isot. 1994; 45:1143–1147.
83. Holland JP, Sheh YC, Lewis JS. Nucl Med Biol. 2009; 36:729–739. [PubMed: 19720285]
84. Obata A, Kasamatsu S, McCarthy DW, Welch MJ, Saji H, Yonekura Y, Fujibayashi Y. Nucl Med Biol. 2003; 30:535–539. [PubMed: 12831992]

85. McCarthy DW, Shefer RE, Klinkowstein RE, Bass LA, Margeneau WH, Cutler CS, Anderson CJ, Welch MJ. Nucl Med Biol. 1997; 24:35–43. [PubMed: 9080473]
86. Avila-Rodriguez MA, Nye JA, Nickles RJ. Appl Radiat Isot. 2007; 65:1115–1120. [PubMed: 17669663]
87. Kim JY, Park H, Lee JC, Kim KM, Lee KC, Ha HJ, Choi TH, An GI, Cheon GJ. Appl Radiat Isot. 2009; 67:1190–1194. [PubMed: 19299153]
88. Le VS, Howse J, Zaw M, Pellegrini P, Katsifis A, Greguric I, Weiner R. Appl Radiat Isot. 2009; 67:1324–1331. [PubMed: 19307129]
89. Kozempel J, Abbas K, Simonelli F, Zampese M, Holzwarth U, Gibson N, Leseticky L. Radiochim Acta. 2007; 95:75–80.
90. Abbas K, Kozempel J, Bonardi M, Groppi F, Alfarano A, Holzwarth U, Simonelli F, Hofman H, Horstmann W, Menapace E, Leseticky L, Gibson N. Appl Radiat Isot. 2006; 64:1001–1005. [PubMed: 16500108]
91. Hilgers K, Stoll T, Skakun Y, Coenen HH, Qaim SM. Appl Radiat Isot. 2003; 59:343–351. [PubMed: 14622933]
92. Van So L, Pellegrini P, Katsifis A, Howse J, Greguric I. J Radioanal Nucl Chem. 2008; 277:451–466.
93. Bakaj M, Zimmer M. J Mol Struct. 1999; 508:59–72.
94. Pasquarello A, Petri I, Salmon PS, Parisel O, Car R, Toth E, Powell DH, Fischer HE, Helm L, Merbach AE. Science. 2001; 291:856–859. [PubMed: 11157161]
95. Delgado R, Felix V, Lima LMP, Price DW. Dalton Trans. 2007:2734–2745. [PubMed: 17592589]
96. Sun X, Kim J, Martell AE, Welch MJ, Anderson CJ. Nucl Med Biol. 2004; 31:1051–1059. [PubMed: 15607487]
97. Smith SV. Q J Nucl Med Mol Imag. 2008; 52:193–202.
98. Sun X, Wuest M, Weisman GR, Wong EH, Reed DP, Boswell CA, Motekaitis R, Martell AE, Welch MJ, Anderson CJ. J Med Chem. 2002; 45:469–477. [PubMed: 11784151]
99. Wadas TJ, Anderson CJ. Nat Protoc. 2006; 1:3062–3068. [PubMed: 17406569]
100. Li WP, Meyer LA, Capretto DA, Sherman CD, Anderson CJ. Cancer Biother Radiopharm. 2008; 23:158–171. [PubMed: 18454685]
101. Wong EH, Weisman GR, Hill DC, Reed DP, Rogers ME, Condon JS, Fagan MA, Calabrese JC, Lam KC, Guzei IA, Rheingold AL. J Am Chem Soc. 2000; 122:10561–10572.
102. Bandoli G, Dolmella A, Tisato F, Porchia M, Refosco F. Coord Chem Rev. 2009; 253:56–77.
103. Weiner RE, Thakur ML. Handbook of Radiopharmaceuticals. 2003:363–399.
104. Francesconi LC, Liu BL, Billings JJ, Carroll PJ, Graczyk G, Kung HF. J Chem Soc, Chem Commun. 1991:94–95.
105. Jarjayes O, Mortini F, d'Hardemare AD, Philouze C, Serratrice G. Eur J Inorg Chem. 2005:4417–4424.
106. Motekaitis RJ, Martell AE, Koch SA, Hwang JW, Quarless DA, Welch MJ. Inorg Chem. 1998; 37:5902–5911.
107. Blend MJ, Stastny JJ, Swanson SM, Brechbiel MW. Cancer Biother Radiopharm. 2003; 18:355–363. [PubMed: 12954122]
108. Li YJ, Martell AE, Hancock RD, Reibenspies JH, Anderson CJ, Welch MJ. Inorg Chem. 1996; 35:404–414. [PubMed: 11666222]
109. Ma R, Motekaitis RJ, Martell AE. Inorg Chim Acta. 1994; 224:151–155.
110. Martell AE, Motekaitis R, Clarke ET, Delgado R, Sun YZ, Ma R. Supramol Chem. 1997; 8:253–253.
111. Fani M, Andre JP, Maecke HR. Contrast Media Mol Imaging. 2008; 3:53–63. [PubMed: 18383455]
112. Eder M, Wangler B, Knackmuss S, LeGall F, Little M, Haberkorn U, Mier W, Eisenhut M. Eur J Nucl Med Mol Imaging. 2008; 35:1878–1886. [PubMed: 18509635]
113. Clarke ET, Martell AE. Inorg Chim Acta. 1991; 181:273–280.

114. Broan CJ, Cox JPL, Craig AS, Kataky R, Parker D, Harrison A, Randall AM, Ferguson G. J Chem Soc, Perkin Trans 2. 1991:87–99.
115. Parker D, Pulukkody K, Smith FC, Batsanov A, Howard JAK. J Chem Soc, Dalton Trans. 1994:689–693.
116. Kumar K, Chang CA, Francesconi LC, Dischino DD, Malley MF, Gougoutas JZ, Tweedle MF. Inorg Chem. 1994; 33:3567–3575.
117. Amin S, Marks C, Toomey LM, Churchill MR, Morrow JR. Inorg Chim Acta. 1996; 246:99–107.
118. Clifford T, Boswell CA, Biddlecombe GB, Lewis JS, Brechbiel MW. J Med Chem. 2006; 49:4297–4304. [PubMed: 16821789]
119. Schiller E, Bergmann R, Pietzsch J, Noll B, Sterger A, Johannsen B, Wunderlich G, Pietzsch HJ. Nucl Med Biol. 2008; 35:227–232. [PubMed: 18312833]
120. Schlesinger J, Koezle I, Bergmann R, Tamburini S, Bolzati C, Tisato F, Noll B, Klussmann S, Vonhoff S, Wuest F, Pietzsch HJ, Steinbach J. Bioconjugate Chem. 2008; 19:928–939.
121. Davidovich RL, Logvinova VB, Teplukhina LV. Koordinatsionnaya Khimiya. 1992; 18:580–584.
122. Pozhidaev AI, Poraikoshits MA, Polynova TN. J Struct Chem. 1974; 15:548–553.
123. Meijs WE, Haisma HJ, Klok RP, van Gog FB, Kievit E, Pinedo HM, Herscheid JDM. J Nucl Med. 1997; 38:112–118. [PubMed: 8998164]
124. Perk LR, Vosjan M, Visser GWM, Budde M, Jurek P, Kiefer GE, van Dongen G. Eur J Nucl Med Mol Imaging. 2010; 37:250–259. [PubMed: 19763566]
125. Holland JP, Divilov V, Bander NH, Smith-Jones PM, Larson SM, Lewis JS. J Nucl Med. 2010; 51:1293–1300. [PubMed: 20660376]
126. Meyer GJ, Macke HR, Schuhmacher J, Knapp WH, Hoffman TJ. Eur J Nucl Med Mol Imaging. 2003; 31:1097–1104. [PubMed: 15029459]
127. Velikyan I, Sundberg AL, Lindhe O, Hoglund AU, Eriksson O, Werner E, Carlsson J, Bergstrom M, Langstrom B, Tolmachev V. J Nucl Med. 2005; 46:1881–1888. [PubMed: 16269603]
128. Dimitrakopoulou-Strauss A, Hohenberger P, Haberkorn U, Macke HR, Eisenhut M, Strauss LG. J Nucl Med. 2007; 48:1245–1250. [PubMed: 17631559]
129. Liu Z, Niu G, Shi J, Liu S, Wang F, Liu S, Chen X. Eur J Nucl Med Mol Imaging. 2009; 36:947–957. [PubMed: 19159928]
130. Wei L, Zhang X, Gallazzi F, Miao Y, Jin X, Brechbiel MW, Xu H, Clifford T, Welch MJ, Lewis JS, Quinn TP. Nucl Med Biol. 2009; 36:345–354. [PubMed: 19423001]
131. Eisenwiener KP, Prata MIM, Buschmann I, Zhang HW, Santos AC, Wenger S, Reubi JC, Macke HR. Bioconjugate Chem. 2002; 13:530–541.
132. Henze M, Schuhmacher J, Hipp P, Kowalski J, Becker DW, Doll J, Macke HR, Hofmann M, Debus J, Haberkorn U. J Nucl Med. 2001; 42:1053–1056. [PubMed: 11438627]
133. Heppeler A, Froidevaux S, Macke HR, Jermann E, Behe M, Powell P, Hennig M. Chem–Eur J. 1999; 5:1974–1981.
134. Hofmann M, Maecke H, Borner AR, Weckesser E, Schoffski P, Oei ML, Schumacher J, Henze M, Heppeler A, Meyer GJ, Knapp WH. Eur J Nucl Med Mol Imaging. 2001; 28:1751–1757.
135. Asti M, De Pietri G, Fraternali A, Grassi E, Sghedoni R, Floroni F, Roesch F, Versari A, Salvo D. Nucl Med Biol. 2008; 35:721–724. [PubMed: 18678358]
136. Lendvai G, Monazzam A, Velikyan I, Eriksson B, Josephsson R, Langstrom B, Bergstrom M, Estrada S. Oligonucleotides. 2009; 19:223–231. [PubMed: 19732020]
137. Roivainen A, Tolvanen T, Salomaki S, Lendvai G, Velikyan I, Numminen P, Valila M, Sipila H, Bergstrom M, Harkonen P, Lonnberg H, Langstrom B. J Nucl Med. 2004; 45:347–355. [PubMed: 14960659]
138. Schlesinger J, Bergmann R, Klussmann S, Wuest F. Lett Drug Des Discovery. 2006; 3:330–335.
139. Anderson CJ, Green MA, Fujibayashi Y. Handbook of Radiopharmaceuticals. 2003:401–422.
140. Mindt TL, Muller C, Stuker F, Salazar JF, Hohn A, Mueggler T, Rudin M, Schibli R. Bioconjugate Chem. 2009; 20:1940–1949.
141. Nwe K, Brechbiel MW. Cancer Biother Radiopharm. 2009; 24:289–301. [PubMed: 19538051]
142. Glaser M, Robins EG. J Labelled Compd Radiopharm. 2009; 52:407–414.

143. Waengler C, Schirrmacher R, Bartenstein P, Waengler B. Curr Med Chem. 2010; 17:1092–1116. [PubMed: 20156157]
144. Wang C, Wang N, Zhou W, Shen YM, Zhang L. Progress in Chemistry. 2010; 22:1591–1602.
145. Glaser M, Solbakken M, Turton DR, Pettitt R, Barnett J, Arukwe J, Karlsen H, Cuthbertson A, Luthra SK, Arstad E. Amino Acids. 2008; 37:717–724. [PubMed: 19011732]
146. Marik J, Sutcliffe JL. Tetrahedron Lett. 2006; 47:6681–6684.
147. Lebedev AY, Holland JP, Lewis JS. Chem Commun. 2009; 46:1706–1708.
148. Knor S, Modlinger A, Poethko T, Schottelius M, Wester HJ, Kessler H. Chem–Eur J. 2007; 13:6082–6090. [PubMed: 17503419]
149. Martin ME, Parameswarappa SG, O'Dorisio MS, Pigge FC, Schultz MK. Bioorg Med Chem Lett. 2010; 20:4805–4807. [PubMed: 20630750]
150. Schultz MK, Parameswarappa SG, Pigge FC. Org Lett. 2010; 12:2398–2401. [PubMed: 20423109]
151. Devaraj NK, Upadhyay R, Hatin JB, Hilderbrand SA, Weissleder R. Angew Chem, Int Ed. 2009; 48:7013–7016.
152. Devaraj NK, Weissleder R, Hilderbrand SA. Bioconjugate Chem. 2008; 19:2297–2299.
153. Tanaka K, Masuyama T, Hasegawa K, Tahara T, Mizuma H, Wada Y, Watanabe Y, Fukase K. Angew Chem, Int Ed. 2008; 47:102–105.
154. Velikyan I, Beyer GJ, Langstrom B. Bioconjugate Chem. 2004; 15:554–560.
155. Putzer D, Gabriel M, Henninger B, Kendler D, Uprimny C, Dobrozemsky G, Decristoforo C, Bale RJ, Jaschke W, Virgolini IJ. J Nucl Med. 2009; 50:1214–1221. [PubMed: 19617343]
156. Parry JJ, Kelly TS, Andrews R, Rogers BE. Bioconjugate Chem. 2007; 18:1110–1117.
157. Nayak TK, Regino CAS, Wong KJ, Milenic DE, Garmestani K, Baidoo KE, Szajek LP, Brechbiel MW. Eur J Nucl Med Mol Imaging. 2010; 37:1368–1376. [PubMed: 20155263]
158. [Accessed October 11, 2010] Brookhaven National Laboratory: National Nuclear Decay Center. 2010. http://www.nndcbnl.gov
159. Welch, MJ.; Redvanly, CS., editors. Handbook of Radiopharmaceuticals: Radiochemistry and Applications. Wiley; New York: 2003.
160. Maecke HR, Andre JP. Ernst Schering Res Found Workshop. 2007; 62:215–242. [PubMed: 17172157]
161. Ehrhardt GJ, Welch MJ. J Nucl Med. 1978; 19:925–929. [PubMed: 98618]
162. Dejesus OT, Nickles RJ. Int J Radiat Appl Instrum, Part A. 1990; 41:789–790.
163. Eary JF, Link JM, Kishore R, Johnson MW, Badger CC, Richter KY, Krohn KA, Nelp WB. J Nucl Med. 1986; 27:983–983.
164. Meijs WE, Herscheid JDM, Haisma HJ, Wijbrandts R, Vanlangevelde F, Vanleuffen PJ, Mooy R, Pinedo HM. Appl Radiat Isot. 1994; 45:1143–1147.
165. Martell, AE.; Smith, RM. Critical Stability Constants. Plenum Press; New York: 1982.
166. Martell, AE.; Hancock, RD. Metal Complexes in Aqueous Solutions. Plenum Press; New York: 1996.
167. Bevilacqua A, Gelb RI, Hebard WB, Zompa LJ. Inorg Chem. 1987; 26:2699–2706.
168. Martell AE, Motekaitis RJ, Clarke ET, Delgado R, Sun YZ, Ma R. Supramol Chem. 1996; 6:353–363.
169. Delgado R, Dasilva JJR. Talanta. 1982; 29:815–822. [PubMed: 18963244]
170. Chaves S, Delgado R, Dasilva J. Talanta. 1992; 39:249–254. [PubMed: 18965370]
171. Woodin KS, Heroux KJ, Boswell CA, Wong EH, Weisman GR, Niu WJ, Tomellini SA, Anderson CJ, Zakharov LN, Rheingold AL. Eur J Inorg Chem. 2005:4829–4833.
172. Bharadwaj PK, Potenza JA, Schugar HJ. J Am Chem Soc. 1986; 108:1351–1352.
173. Bernhardt PV, Bramley R, Engelhardt LM, Harrowfield JM, Hockless DCR, Korybutdaszkiewicz BR, Krausz ER, Morgan T, Sargeson AM, Skelton BW, White AH. Inorg Chem. 1995; 34:3589–3599.
174. Delgado R, Figueira MD, Quintino S. Talanta. 1997; 45:451–462. [PubMed: 18967026]
175. Smith, RM.; Martell, AE. Critical Stability Constants. Plenum Press; New York: 1989.

176. Ma R, Motekaitis RJ, Martell AE. Inorg Chim Acta. 1994; 224:151–155.
177. Motekaitis RJ, Sun YZ, Martell AE. Inorg Chem. 1991; 30:1554–1556.
178. Delgado R, Sun YZ, Motekaitis RJ, Martell AE. Inorg Chem. 1993; 32:3320–3326.
179. Terova, O. University of New Hampshire; 2008.
180. Evers A, Hancock RD, Martell AE, Motekaitis RJ. Inorg Chem. 1989; 28:2189–2195.
181. Martell, AE.; Smith, RM. Critical Stability Constants, Vol 1: Amino Acids. Plenum Press; New York: 1974.
182. Koudelkova M, Vinsova H, Jedinakova-Krizova V. Czech J Phys. 2003; 53:A769–A775.
183. Kodama M, Koike T, Mahatma AB, Kimura E. Inorg Chem. 1991; 30:1270–1273.
184. Bottari E, Anderegg G. Helv Chim Acta. 1967; 50:2349–2355.
185. Ujula T, Salomaki S, Virsu P, Lankinen P, Makinen TJ, Autio A, Yegutkin GG, Knuuti J, Jalkanen S, Roivainen A. Nucl Med Biol. 2009; 36:631–641. [PubMed: 19647169]
186. Schuhmacher J, Zhang HW, Doll J, Macke HR, Matys R, Hauser H, Henze M, Haberkorn U, Eisenhut M. J Nucl Med. 2005; 46:691–699. [PubMed: 15809493]
187. Maschauer S, Einsiedel J, Hocke C, Hubner H, Kuwert T, Gmeiner P, Prante O. ACS Med Chem Lett. 2010; 1:224–228.
188. Wild D, Schmitt JS, Ginj M, Macke HR, Bernard BF, Krenning E, de Jong M, Wenger S, Reubi JC. Eur J Nucl Med Mol Imaging. 2003; 30:1338–1347. [PubMed: 12937948]
189. de Jong J, Bakker W, Krenning E, Breeman WAP, Van Der Pluijm ME, Bernard BF, Visser TJ, Jermann E, Behe M, Powell P, Macke HR. Eur J Nucl Med Mol Imaging. 1997; 24:368–371.
190. Zhang HW, Chen JH, Waldherr C, Hinni K, Waser B, Reubi JC, Maecke HR. Cancer Res. 2004; 64:6707–6715. [PubMed: 15374988]
191. Zhang HW, Schuhmacher J, Waser B, Wild D, Eisenhut M, Reubi JC, Maecke HR. Eur J Nucl Med Mol Imaging. 2007; 34:1198–1208. [PubMed: 17262215]
192. Froidevaux S, Calame-Christe M, Schuhmacher J, Tanner H, Saffrich R, Henze M, Eberle AN. J Nucl Med. 2004; 45:116–123. [PubMed: 14734683]
193. Froidevaux S, Calame-Christe M, Tanner H, Sumanovski L, Eberle AN. J Nucl Med. 2002; 43:1699–1706. [PubMed: 12468522]
194. Eder M, Krivoshein AV, Backer M, Backer JM, Haberkorn U, Eisenhut M. Nucl Med Biol. 2010; 37:405–412. [PubMed: 20447550]
195. Backer MV, Levashova Z, Patel V, Jehning BT, Claffey K, Blankenberg FG, Backer JM. Nat Med. 2007; 13:504–509. [PubMed: 17351626]
196. Liu ZF, Yan YJ, Liu SL, Wang F, Chen XY. Bioconjugate Chem. 2009; 20:1016–1025.
197. Jeong JM, Hong MK, Chang YS, Lee YS, Kim YJ, Cheon GJ, Lee DS, Chung JK, Lee MC. J Nucl Med. 2008; 49:830–836. [PubMed: 18413379]
198. Smithjones PM, Stolz B, Bruns C, Albert R, Reist HW, Fridrich R, Macke HR. J Nucl Med. 1994; 35:317–325. [PubMed: 8295005]
199. Hnatowich DJ, Layne WW, Childs RL. Int J Appl Radiat Isot. 1982; 33:327–332. [PubMed: 7095875]
200. Moerlein SM, Daugherty A, Sobel BE, Welch MJ. J Nucl Med. 1991; 32:300–307. [PubMed: 1992034]
201. Wagner SJ, Welch MJ. J Nucl Med. 1979; 20:428–433. [PubMed: 120419]
202. Eder M, Knackmuss S, Le Gall F, Reusch U, Rybin V, Little M, Haberkorn U, Mier W, Eisenhut M. Eur J Nucl Med Mol Imaging. 2010; 37:1397–1407. [PubMed: 20157706]
203. Smith-Jones PM, Vallabahajosula S, Goldsmith SJ, Navarro V, Hunter CJ, Bastidas D, Bander NH. Cancer Res. 2000; 60:5237–5243. [PubMed: 11016653]
204. Smith-Jones PM, Solit DB, Akhurst T, Alfroze F, Rosen N, Larson SM. Nat Biotechnol. 2004; 22:701–706. [PubMed: 15133471]
205. Smith-Jones PM, Solit DB, Afroze F, Rosen N, Larson SM. J Nucl Med. 2006; 47:793–796. [PubMed: 16644749]
206. Baum RP, Prasad V, Muller D, Schuchardt C, Orlova A, Wennborg A, Tolmachev V, Feldwisch J. J Nucl Med. 2010; 51:892–897. [PubMed: 20484419]

207. Orlova A, Tolmachev V, Pehrson R, Lindborg M, Tran T, Sandstrom M, Nilsson FY, Wennborg A, Abrahmsen L, Feldwisch J. Cancer Res. 2007; 67:2178–2186. [PubMed: 17332348]
208. Tolmachev V, Velikyan I, Sandstrom M, Orlova A. Eur J Nucl Med Mol Imaging. 2010; 37:1356–1367. [PubMed: 20130858]
209. Otsuka FL, Welch MJ, Kilbourn MR, Dence CS, Dilley WG, Wells SA. Int J Radiat Appl Instrum, Part A. 1991; 18:813–816.
210. Otsuka FL, Cance WG, Dilley WG, Scott RW, Davie JM, Wells SA, Welch MJ. Int J Radiat Appl Instrum, Part A. 1988; 15:305–311.
211. Koop B, Reske SN, Neumaier B. Radiochim Acta. 2007; 95:39–42.
212. Tian XB, Aruva MR, Zhang KJ, Shanthly N, Cardi CA, Thakur ML, Wickstrom E. J Nucl Med. 2007; 48:1699–1707. [PubMed: 17909257]
213. Sun XK, Fang HF, Li XX, Rossin R, Welch MJ, Taylor JS. Bioconjugate Chem. 2005; 16:294–305.
214. Lendvai G, Velikyan I, Bergstrom M, Estrada S, Laryea D, Valila M, Salomaki S, Langstrom B. Eur J Pharm Sci. 2005; 26:26–38. [PubMed: 15941654]
215. Tian XB, Chakrabarti A, Amirkhanov NV, Aruva MR, Zhang KJ, Mathew B, Cardi C, Qin WY, Sauter ER, Thakur ML, Wickstrom E. Tumor Progression and Therapeutic Resistance. 2005; 1059:106–144.
216. Rogers BE, Bigott HM, McCarthy DW, Della Manna D, Kim J, Sharp TL, Welch MJ. Bioconjugate Chem. 2003; 14:756–763.
217. Parry JJ, Andrews R, Rogers BE. Breast Cancer Res Treat. 2007; 101:175–183. [PubMed: 16838112]
218. Edwards WB, Xu B, Akers W, Cheney PP, Liang K, Rogers BE, Anderson CJ, Achilefu S. Bioconjugate Chem. 2008; 19:192–200.
219. Chen JQ, Cheng Z, Owen NK, Hoffman TJ, Miao YB, Jurisson SS, Quinn TP. J Nucl Med. 2001; 42:1847–1855. [PubMed: 11752084]
220. McQuade P, Miao YB, Yoo J, Quinn TP, Welch MJ, Lewis JS. J Med Chem. 2005; 48:2985–2992. [PubMed: 15828837]
221. Garrison JC, Rold TL, Sieckman GL, Figueroa SD, Volkert WA, Jurisson SS, Hoffman TJ. J Nucl Med. 2007; 48:1327–1337. [PubMed: 17631556]
222. Hausner SH, Kukis DL, Gagnon MKJ, Stanecki CE, Ferdani R, Marshall JF, Anderson CJ, Sutcliffe JL. Mol Imaging. 2009; 8:111–121. [PubMed: 19397856]
223. Biddlecombe GB, Rogers BE, de Visser M, Parry JJ, de Jong M, Erion JL, Lewis JS. Bioconjugate Chem. 2007; 18:724–730.
224. Chen XY, Liu S, Hou YP, Tohme M, Park R, Bading JR, Conti PS. Mol Imaging Biol. 2004; 6:350–359. [PubMed: 15380745]
225. Chen XY, Hou YP, Tohme M, Park R, Khankaldyyan V, Gonzales-Gomez I, Bading JR, Laug WE, Conti PS. J Nucl Med. 2004; 45:1776–1783. [PubMed: 15471848]
226. Lee HY, Li Z, Chen K, Hsu AR, Xu CJ, Xie J, Sun SH, Chen XY. J Nucl Med. 2008; 49:1371–1379. [PubMed: 18632815]
227. Wu Y, Zhang XZ, Xiong ZM, Cheng Z, Fisher DR, Liu S, Gambhir SS, Chen XY. J Nucl Med. 2005; 46:1707–1718. [PubMed: 16204722]
228. Li ZB, Cai WB, Cao QZ, Chen K, Wu ZH, He LN, Chen XY. J Nucl Med. 2007; 48:1162–1171. [PubMed: 17574975]
229. Chen XY, Park R, Hou YP, Tohme M, Shahinian AH, Bading JR, Conti PS. J Nucl Med. 2004; 45:1390–1397. [PubMed: 15299066]
230. Cai WB, Chen K, Mohamedali KA, Cao QZ, Gambhir SS, Rosenblum MG, Chen XY. J Nucl Med. 2006; 47:2048–2056. [PubMed: 17138749]
231. Wang H, Cai WB, Chen K, Li ZB, Kashefi A, He L, Chen XY. Eur J Nucl Med Mol Imaging. 2007; 34:2001–2010. [PubMed: 17694307]
232. Li ZB, Niu G, Wang H, He L, Yang L, Ploug M, Chen XY. Clin Cancer Res. 2008; 14:4758–4766. [PubMed: 18676745]

233. Cao Q, Cai W, Niu G, He L, Chen X. Clin Cancer Res. 2008; 14:6137–6145. [PubMed: 18829492]
234. Cheng Z, Xiong ZM, Subbarayan M, Chen XY, Gambhir SS. Bioconjugate Chem. 2007; 18:765–772.
235. Jiang L, Kimura RH, Miao Z, Silverman AP, Ren G, Liu HG, Li PY, Gambhir SS, Cochran JR, Cheng Z. J Nucl Med. 2010; 51:251–258. [PubMed: 20124048]
236. Kimura RH, Cheng Z, Gambhir SS, Cochran JR. Cancer Res. 2009; 69:2435–2442. [PubMed: 19276378]
237. Liu YJ, Abendschein D, Woodard GE, Rossin R, McCommis K, Zheng J, Welch MJ, Woodard PK. J Nucl Med. 2010; 51:85–91. [PubMed: 20008978]
238. Rossin R, Muro S, Welch MJ, Muzykantov VR, Schuster DP. J Nucl Med. 2008; 49:103–111. [PubMed: 18077519]
239. Liu DJ, Overbey D, Watkinson LD, Smith CJ, Daibes-Figueroa S, Hoffman TJ, Forte LR, Volkert WA, Giblin MF. Bioconjugate Chem. 2010; 21:1171–1176.
240. Locke LW, Chordia MD, Zhang Y, Kundu B, Kennedy D, Landseadel J, Xiao L, Fairchild KD, Berr SS, Linden J, Pan DF. J Nucl Med. 2009; 50:790–797. [PubMed: 19372473]
241. Levashova Z, Backer MV, Horng G, Felsher D, Backer JM, Blankenberg FG. Bioconjugate Chem. 2009; 20:742–749.
242. Vavere AL, Biddlecombe GB, Spees WM, Garbow JR, Wijesinghe D, Andreev OA, Englenman DM, Reshetnyak YK, Lewis JS. Cancer Res. 2009; 69:4510–4516. [PubMed: 19417132]
243. Wei LH, Butcher C, Miao YB, Gallazzi F, Quinn TP, Welch MJ, Lewis JS. J Nucl Med. 2007; 48:64–72. [PubMed: 17204700]
244. Wadas TJ, Eiblmaier M, Zheleznyak A, Sherman CD, Ferdani R, Liang K, Achilefu S, Anderson CJ. J Nucl Med. 2008; 49:1819–1827. [PubMed: 18927338]
245. Sprague ES, Peng Y, Sun X, Weisman GR, Wong EH, Achilefu S, Anderson CJ. Clin Cancer Res. 2004; 10:8674–8682. [PubMed: 15623652]
246. DeNardo SJ, Liu R, Albrecht H, Natarajan A, Sutcliffe JL, Anderson C, Peng L, Ferdani R, Cherry SR, Lam KS. J Nucl Med. 2009; 50:625–634. [PubMed: 19289419]
247. Wei L, Ye Y, Wadas TJ, Lewis JS, Welch MJ, Achilefu S, Anderson CJ. Nucl Med Biol. 2009; 36:277–285. [PubMed: 19324273]
248. Sprague JE, Kitaura H, Zou W, Ye YP, Achilefu S, Weilbaecher KN, Teitelbaum SL, Anderson CJ. J Nucl Med. 2007; 48:311–318. [PubMed: 17268030]
249. Anderson CJ, Pajeau TS, Edwards WB, Sherman ELC, Rogers BE, Welch MJ. J Nucl Med. 1995; 36:2315–2325. [PubMed: 8523125]
250. Anderson CJ, Jones LA, Bass LA, Sherman ELC, McCarthy DW, Cutler PD, Lanahan MV, Cristel ME, Lewis JS, Schwarz SW. J Nucl Med. 1998; 39:1944–1951. [PubMed: 9829587]
251. Lewis JS, Lewis MR, Cutler PD, Srinivasan A, Schmidt MA, Schwarz SW, Morris MM, Miller JP, Anderson CJ. Clin Cancer Res. 1999; 5:3608–3616. [PubMed: 10589778]
252. Lewis JS, Lewis MR, Srinivasan A, Schmidt MA, Wang J, Anderson CJ. J Med Chem. 1999; 42:1341–1347. [PubMed: 10212119]
253. Lewis JS, Srinivasan A, Schmidt MA, Anderson CJ. Nucl Med Biol. 1999; 26:267–273. [PubMed: 10363797]
254. Edwards WB, Anderson CJ, Fields GB, Welch MJ. Bioconjugate Chem. 2001; 12:1057–1065.
255. Prasanphanich AF, Nanda PK, Rold TL, Ma LX, Lewis MR, Garrison JC, Hoffman TJ, Sieckman GL, Figueroa SD, Smith CJ. Proc Natl Acad Sci USA. 2007; 104:12462–12467. [PubMed: 17626788]
256. Prasanphanich AF, Retzloff L, Lane SR, Nanda PK, Sieckman GL, Rold TL, Ma LX, Figueroa SD, Sublett SV, Hoffman TJ, Smith CJ. Nucl Med Biol. 2009; 36:171–181. [PubMed: 19217529]
257. Thakur ML, Aruva MR, Gariepy J, Acton P, Rattan S, Prasad S, Wickstrom E, Alavi A. J Nucl Med. 2004; 45:1381–1389. [PubMed: 15299065]
258. Zhang K, Aruva MR, Shanthly N, Cardi CA, Rattan S, Patel C, Kim C, McCue PA, Wickstrom E, Thakur ML. J Nucl Med. 2008; 49:112–121. [PubMed: 18077536]

259. Gasser G, Tjioe L, Graham B, Belousoff MJ, Juran S, Walther M, Kunstler JU, Bergmann R, Stephan H, Spiccia L. Bioconjugate Chem. 2008; 19:719–730.
260. Cai HC, Fissekis J, Conti PS. Dalton Trans. 2009:5395–5400. [PubMed: 19565091]
261. Cai HC, Li ZB, Huang CW, Shahinian AH, Wang H, Park R, Conti PS. Bioconjugate Chem. 2010; 21:1417–1424.
262. Cheng Z, De Jesus OP, Kramer DJ, De A, Webster JM, Gheysens O, Levi J, Namavari M, Wang S, Park JM, Zhang R, Liu H, Lee B, Syud FA, Gambhir SS. Mol Imaging Biol. 2010; 12:316–324. [PubMed: 19779897]
263. Olafsen T, Kenanova VE, Sundaresan G, Anderson AL, Crow D, Yazaki PJ, Li L, Press MF, Gambhir SS, Williams LE, Wong JYC, Raubitschek AA, Shively JE, Wu AM. Cancer Res. 2005; 65:5907–5916. [PubMed: 15994969]
264. Lewis MR, Kao JY, Anderson ALJ, Shively JE, Raubitschek A. Bioconjugate Chem. 2001; 12:320–324.
265. Niu G, Cai WB, Chen K, Chen XY. Mol Imaging Biol. 2008; 10:99–106. [PubMed: 18157579]
266. Niu G, Li Z, Xie J, Le QT, Chen X. J Nucl Med. 2009; 50:1116–1123. [PubMed: 19525473]
267. Paudyal P, Paudyal B, Hanaoka H, Oriuchi N, Iida Y, Yoshioka H, Tominaga H, Watanabe S, Ishioka NS, Endo K. Cancer Sci. 2010; 101:1045–1050. [PubMed: 20219072]
268. Li L, Bading J, Yazaki PJ, Ahuja AH, Crow D, Colcher D, Williams LE, Wong JYC, Raubitschek A, Shively JE. Bioconjugate Chem. 2008; 19:89–96.
269. Li L, Turatti F, Crow D, Bading JR, Anderson AL, Poku E, Yazaki PJ, Williams LE, Tamvakis D, Sanders P, Leong D, Raubitschek A, Hudsony PJ, Colcher D, Shively JE. J Nucl Med. 2010; 51:1139–1146. [PubMed: 20554731]
270. Martin SM, O'Donnell RT, Kukis DL, Abbey CK, McKnight H, Sutcliffe JL, Tuscano JM. Mol Imaging Biol. 2008; 11:79–87. [PubMed: 18949521]
271. Elsasser-Beile U, Reischl G, Wiehr S, Buhler P, Wolf P, Alt K, Shively J, Judenhofer MS, Machulla HJ, Pichler BJ. J Nucl Med. 2009; 50:606–611. [PubMed: 19289418]
272. Li WP, Meyer LA, Capretto DA, Sherman CD, Anderson CJ. Cancer Biother Radiopharm. 2008; 23:158–171. [PubMed: 18454685]
273. Zimmermann K, Grunberg J, Honer M, Ametamey S, Schubiger PA, Novak-Hofer I. Nucl Med Biol. 2003; 30:417–427. [PubMed: 12767399]
274. Smith-Jones P, Fridrich R, Kaden TA, Novak-Hofer I, Siebold K, Tschudin D, Maecke H. Bioconjugate Chem. 1991; 2:415–421.
275. Anderson CJ, Schwarz SW, Connett JM, Cutler PD, Guo LW, Germain CJ, Philpott GW, Zinn KR, Greiner DP, Meares CF, Welch MJ. J Nucl Med. 1995; 36:850–858. [PubMed: 7738663]
276. Milenic DE, Wong KJ, Baidoo KE, Ray GL, Garmestani K, Williams M, Brechbiel MW. Cancer Biother Radiopharm. 2008; 23:619–631. [PubMed: 18999934]
277. Nayak TK, Garmestani K, Baidoo KE, Milenic DE, Brechbiel MW. J Nucl Med. 2010; 51:942–950. [PubMed: 20484421]
278. Ray GL, Baidoo KE, Wong KJ, Williams M, Garmestani K, Brechbiel MW, Milenic DE. Br J Pharmacol. 2009; 157:1541–1548. [PubMed: 19681874]
279. Lovqvist A, Humm JL, Sheikh A, Finn RD, Koziorowski J, Ruan S, Pentlow KS, Jungbluth A, Welt S, Lee FT, Brechbiel MW, Larson SM. J Nucl Med. 2001; 42:1281–1287. [PubMed: 11483692]
280. Clarke K, Lee FT, Brechbiel MW, Smyth FE, Old LJ, Scott AM. Cancer Res. 2000; 60:4804–4811. [PubMed: 10987290]
281. Nikula TK, Curcio MJ, Brechbiel MW, Gansow OA, Finn RD, Scheinberg DA. Nucl Med Biol. 1995; 22:387–390. [PubMed: 7627155]
282. Schneider DW, Heitner T, Alicke B, Light DR, McLean K, Satozawa N, Parry G, Yoo J, Lewis JS, Parry R. J Nucl Med. 2009; 50:435–443. [PubMed: 19223400]
283. Wei L, Zhang X, Gallazzi F, Miao Y, Jin X, Brechbiel MW, Xu H, Clifford T, Welch MJ, Lewis JS, Quinn TP. Nucl Med Biol. 2009; 36:345–354. [PubMed: 19423001]
284. Breeman WAP, De Jong M, Bernard BF, Kwekkeboom DJ, Srinivasan A, Van Der Pluijm ME, Hofland LJ, Visser TJ, Krenning EP. Int J Cancer. 1999; 83:657–663. [PubMed: 10521803]

285. Breeman WAP, de Jong M, Erion JL, Bugaj JE, Srinivasan A, Bernard BF, Kwekkeboom DJ, Visser TJ, Krenning EP. J Nucl Med. 2002; 43:1650–1656. [PubMed: 12468515]

286. Cheng Z, Chen JQ, Miao YB, Owen NK, Quinn TP, Jurisson SS. J Med Chem. 2002; 45:3048–3056. [PubMed: 12086490]

287. Albert R, Smith-Jones P, Stolz B, Simeon C, Knecht H, Bruns C, Pless J. Bioorg Med Chem Lett. 1998; 8:1207–1210. [PubMed: 9871736]

288. Rosch F, Herzog H, Stolz B, Brockmann J, Kohle M, Muhlensiepen H, Marbach P, Muller-Gartner HW. Eur J Nucl Med Mol Imaging. 1999; 26:358–366.

289. Meijs WE, Haisma HJ, Klok RP, van Gog FB, Kievit E, Pinedo HM, Herscheid JDM. J Nucl Med. 1997; 38:112–118. [PubMed: 8998164]

290. Verel I, Visser GWM, Boellaard R, Boerman OC, van Eerd J, Snow GB, Lammertsma AA, van Dongen G. J Nucl Med. 2003; 44:1663–1670. [PubMed: 14530484]

291. Borjesson PKE, Jauw YWS, de Bree R, Roos JC, Castelijns JA, Leemans CR, van Dongen G, Boellaard R. J Nucl Med. 2009; 50:1828–1836. [PubMed: 19837762]

292. Perk LR, Walsum MSV, Visser GWM, Kloet RW, Vosjan M, Leemans CR, Giaccone G, Albano R, Comoglio PM, van Dongen G. Eur J Nucl Med Mol Imaging. 2008; 35:1857–1867. [PubMed: 18491091]

293. Perk LR, Visser GWM, Vosjan M, Stigter-van Walsum M, Tijink BM, Leemans CR, van Dongen G. J Nucl Med. 2005; 46:1898–1906. [PubMed: 16269605]

294. Aerts H, Dubois L, Perk L, Vermaelen P, van Dongen G, Wouters BG, Lambin P. J Nucl Med. 2009; 50:123–131. [PubMed: 19091906]

295. Nagengast WB, de Vries EG, Hospers GA, Mulder NH, de Jong JR, Hollema H, Brouwers AH, van Dongen GA, Perk LR, Lub-de Hooge MN. J Nucl Med. 2007; 48:1313–1319. [PubMed: 17631557]

296. Nagengast WB, de Korte MA, Munnink THO, Timmer-Bosscha H, den Dunnen WF, Hollema H, de Jong JR, Jensen MR, Quadt C, Garcia-Echeverria C, van Dongen GAMS, Lub-de Hooge MN, Schroder CP, de Vries EGE. J Nucl Med. 2010; 51:761–767. [PubMed: 20395337]

297. Perk LR, Visser OJ, Walsum MSV, Vosjan M, Visser GWM, Zijlstra JM, Huijgens PC, van Dongen G. Eur J Nucl Med Mol Imaging. 2006; 33:1337–1345. [PubMed: 16832633]

298. Munnink THO, de Korte MA, Nagengast WB, Timmer-Bosscha H, Schroder CP, de Jong JR, van Dongen G, Jensen MR, Quadt C, Lub-de Hooge MN, de Vries EGE. Eur J Cancer. 2010; 46:678–684. [PubMed: 20036116]

299. Munnink TO, Dijkers E, Hooge ML, Kosterink J, Brouwers A, de Jong J, van Dongen G, de Vries E. J Clin Oncol. 2009; 27:1045.

300. Brouwers A, Verel I, Van Eerd J, Visser G, Steffens M, Oosterwijk E, Corstens F, Oyen W, Van Dongen G, Boerman O. Cancer Biother Radiopharm. 2004; 19:155–163. [PubMed: 15186595]

301. Hoeben BAW, Kaanders J, Franssen GM, Troost EGC, Rijken P, Oosterwijk E, van Dongen G, Oyen WJG, Boerman OC, Bussink J. J Nucl Med. 2010; 51:1076–1083. [PubMed: 20554724]

302. Holland JP, Caldas-Lopes E, Divilov V, Longo VA, Taldone T, Zatorska D, Chiosis G, Lewis JS. Plos One. 2010; 5

303. Ruggiero A, Holland JP, Lewis JS, Grimm J. J Nucl Med. 2010; 51:1123–1130. [PubMed: 20554722]

304. Vosjan M, Perk LR, Visser GWM, Budde M, Jurek P, Kiefer GE, van Dongen G. Nat Protoc. 2010; 5:739–743. [PubMed: 20360768]

305. Tinianow JN, Gill HS, Ogasawara A, Flores JE, Vanderbilt AN, Luis E, Vandlen R, Darwish M, Junutula JR, Williams SP, Marik J. Nucl Med Biol. 2010; 37:289–297. [PubMed: 20346868]

Biographies

Brian M. Zeglis, Ph.D.

Dr. Brian Zeglis received his B.S. in chemistry summa cum laude from Yale University (2004), where he worked under the guidance of Professor Robert H. Crabtree. For his graduate studies, he attended the California Institute of Technology as an NSF pre-doctoral fellow. At Caltech, Brian worked under the mentorship of Professor Jacqueline K. Barton, studying the synthesis and development of DNA-binding octahedral metal complexes. After receiving his Ph.D. (2009), Brian moved to Memorial Sloan-Kettering Cancer Center, where he works as an NIH post-doctoral fellow in the laboratory of Professor Jason S. Lewis. Currently, his research is focused on the design, synthesis, and evaluation of ^{64}Cu- and ^{89}Zr-based PET radiopharmaceuticals.

Jason S. Lewis, Ph.D.

Professor Lewis earned a B.Sc. Hons (1992) and an M.Sc. (1993) in Chemistry from the University of Essex. He received a Ph.D. in Biochemistry (1996) from the University of Kent at Canterbury. Following his postdoctoral study at the Washington University School of Medicine, he joined the Radiology faculty (2003). In 2008, he moved to Memorial Sloan-Kettering Cancer Center (New York) where he is currently a Member (with tenure) and Vice Chairman for Basic Research, Chief Attending Radiochemist, and Director of the Cyclotron Core. He holds joint appointments at the Sloan-Kettering Institute, Weill Cornell Medical College and Gerstner Sloan-Kettering Graduate School. Professor Lewis has co-authored over 110 peer-reviewed journal articles, reviews and book chapters.

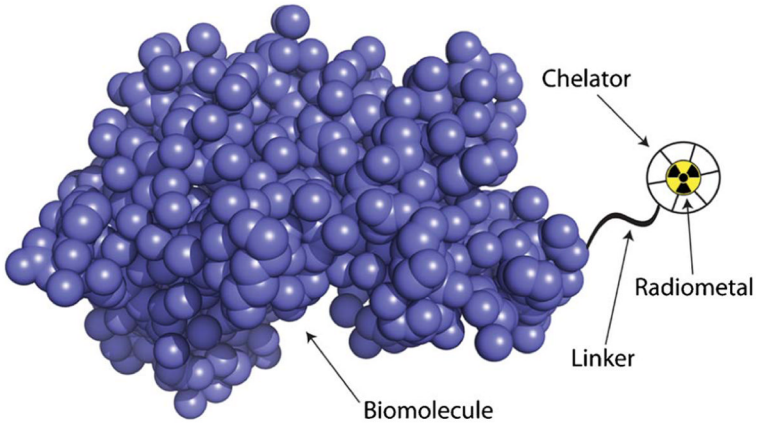

Fig. 1.
The anatomy of a PET bioconjugate.

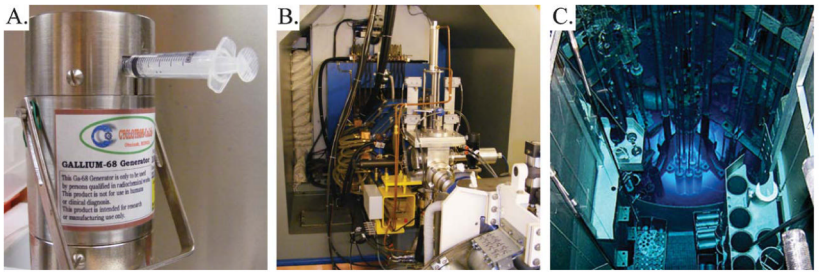

Fig. 2.

Three methods for the production of radionuclides: (A) ^{68}Ga generator, (B) cyclotron, and (C) nuclear reactor. The authors acknowledge David Nickolaus of the Missouri University Research Reactor for the photo of the nuclear reactor.

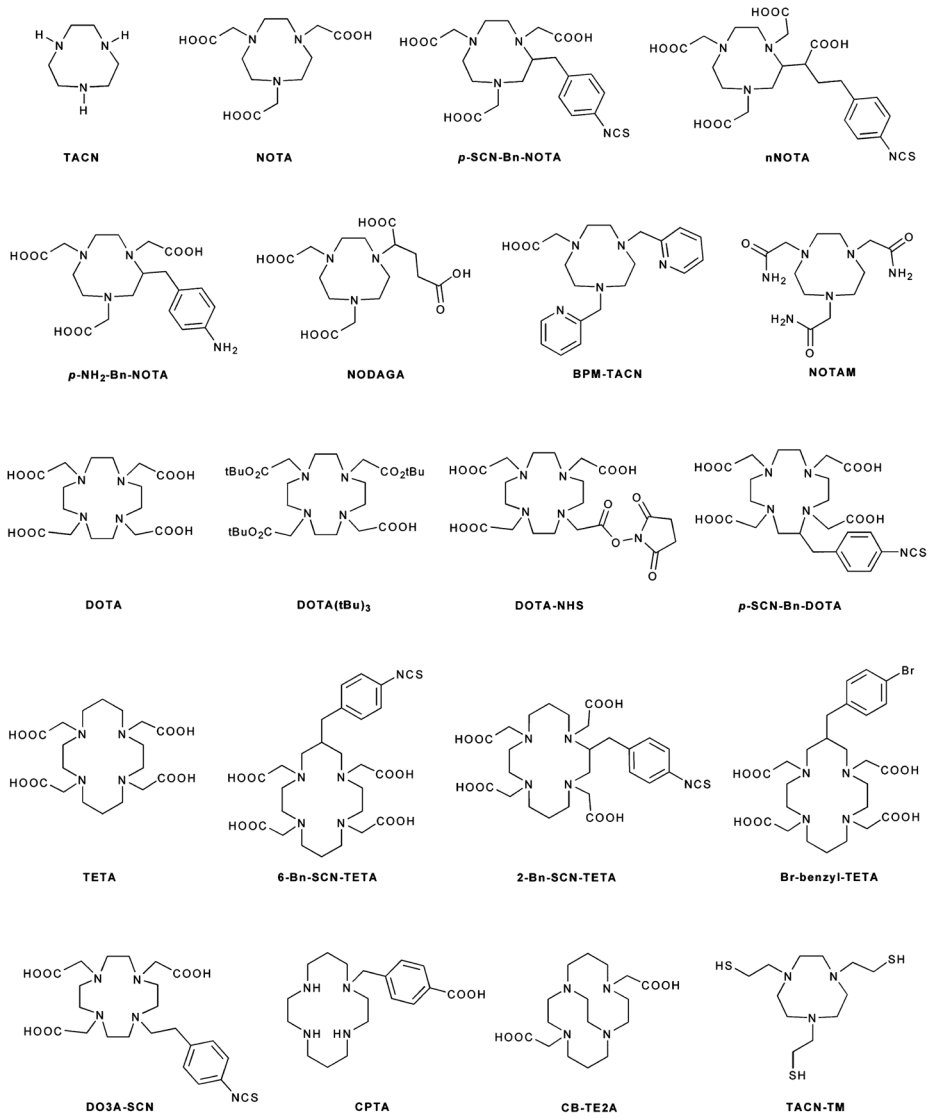

Fig. 3.
Selected chelators and bifunctional chelators for ^{64}Cu, ^{68}Ga, ^{86}Y, and ^{89}Zr.

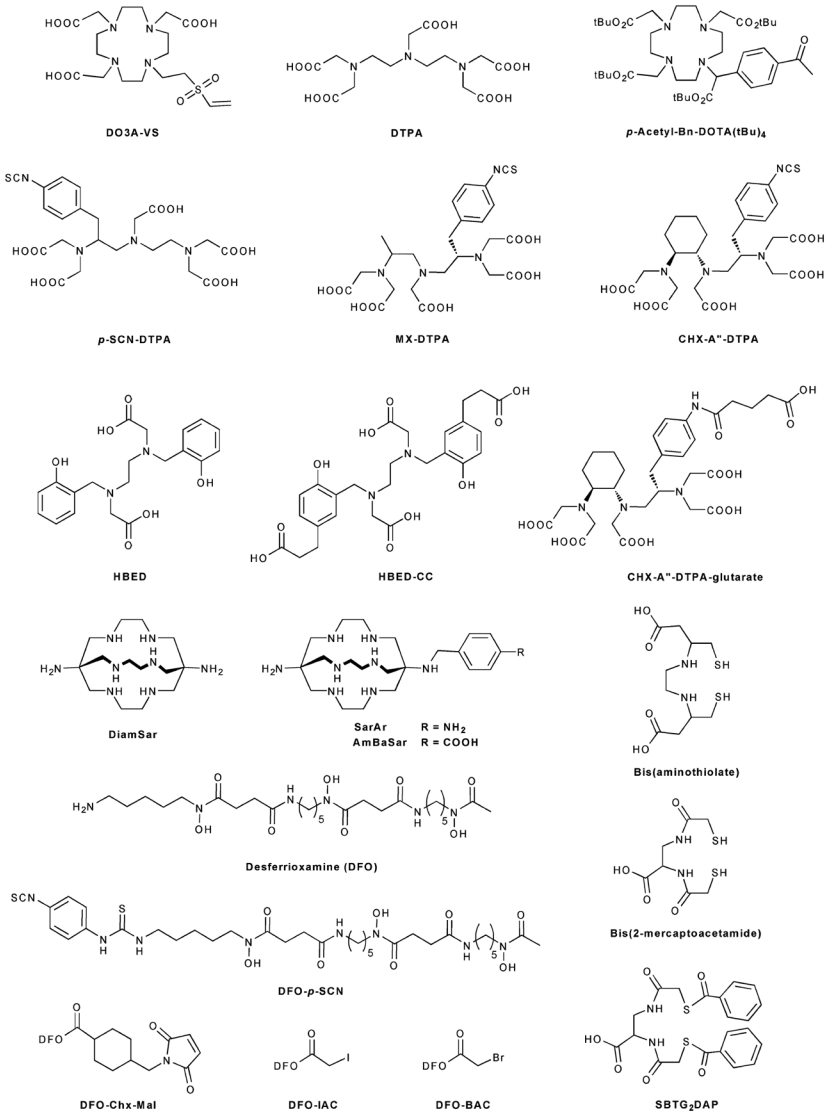

Fig. 4.
Selected chelators and bifunctional chelators for ^{64}Cu, ^{68}Ga, ^{86}Y, and ^{89}Zr.

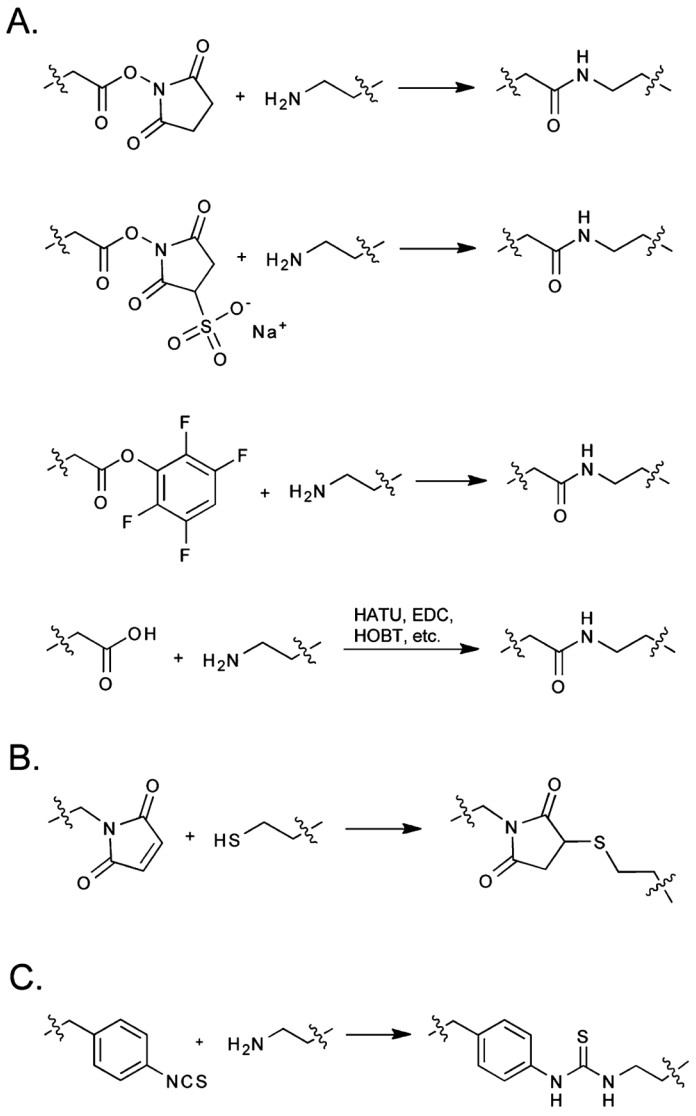

Fig. 5.

The three principal types of bioconjugation reactions: (A) peptide bond formation *via* reaction of a primary amine with a carboxylic acid activated with a succinimidyl ester (NHS), a sulfosuccinimidyl ester (SNHS), tetrafluorophenol (TFP), or a peptide coupling reagent (*e.g.* HATU, HOBT, *etc.*); (B) thioether bond formation *via* reaction of a thiol and a maleimide; and (C) thiourea bond formation *via* reaction of an isothiocyanate and a primary amine.

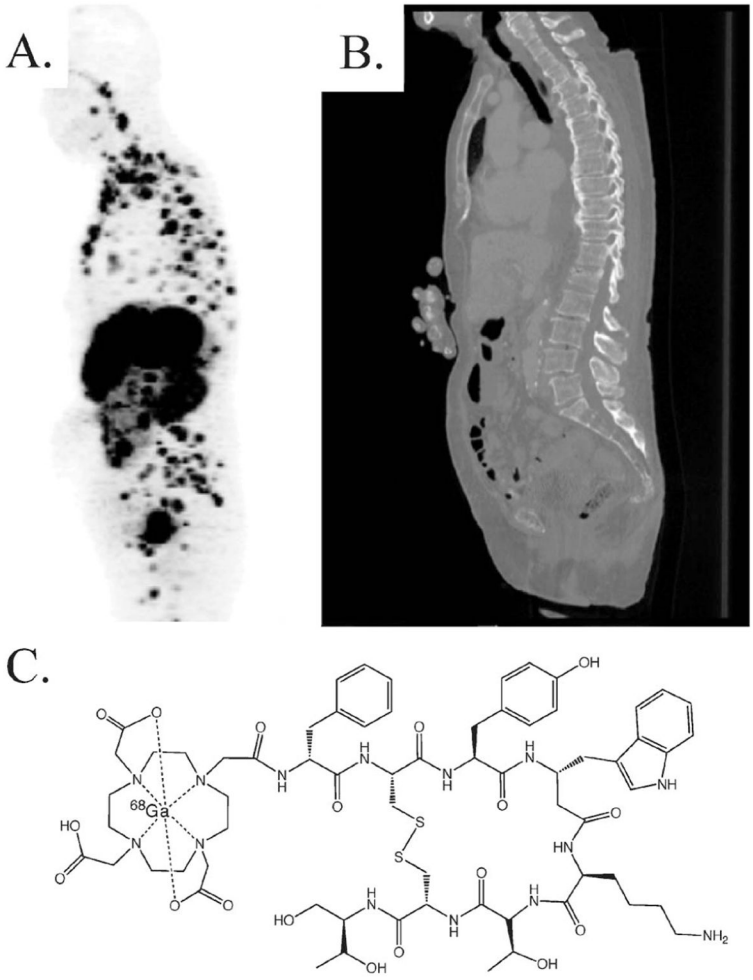

Fig. 6.

A 78-year-old woman with neuroendocrine tumor of unknown primary origin: (A) ^{68}Ga-DOTATOC PET depicts diffuse bone metastases, (B) CT shows only part of widespread bone involvement, and (C) the structure of ^{68}Ga-DOTATOC. Reprinted by permission of the Society of Nuclear Medicine from: D. Putzer, M. Gabriel, B. Henninger, D. Kendler, C. Uprimny, G. Dobrozemsky, C. Decristoforo, R. J. Bale, W. Jaschke and I. J. Virgolini, *Journal of Nuclear Medicine*, 2009, **50**, 1214–1221. Fig. 2.[155]

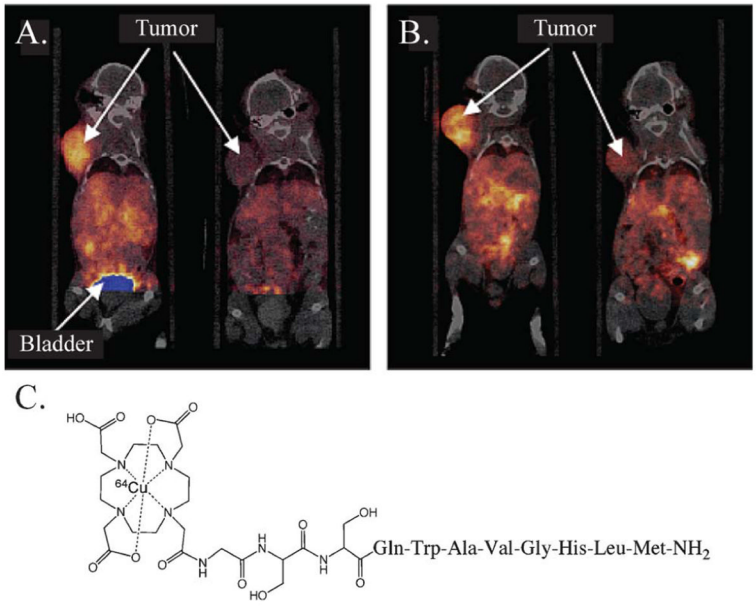

Fig. 7.

Coronal microPET images with co-registered CT of mice bearing PC-3 xenografts in the axillary thorax at (A) 1 h and (B) 24 h. The mice were injected *i.v.* with a GRPR-targeting ^{64}Cu-bombesin analogue, ^{64}Cu-DOTA-GSS-BN(7–14). The mice on the left (A) were not injected with blocking agent, while the mice on the right (B) received 100 μg of Tyr^{4}-BN as an inhibitor. Adapted with permission from J. J. Parry, T. S. Kelly, R. Andrews and B. E. Rogers, *Bioconjugate Chemistry*, 2007, **18**, 1110–1117.[156] Copyright 2007 American Chemical Society.

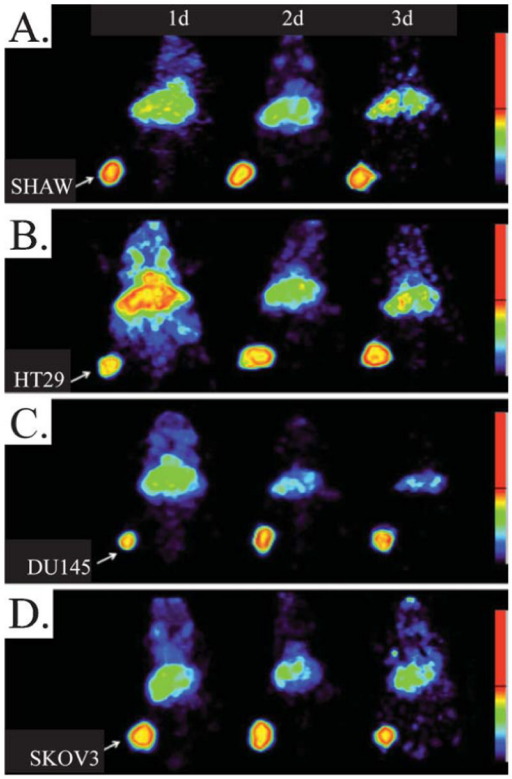

Fig. 8.

Representative reconstructed and processed maximum intensity projections of female athymic (NCr) nu/nu mice bearing (A) SHAW, (B) HT29, (C) DU145, and (D) SKOV3 tumor xenografts injected *i.v.* with 3.8–4.0 MBq of ^{86}Y-CHX-A″-DTPA-cetuximab. Arrows indicate tumors. The scaling is based on % maximum and minimum threshold intensity without normalization to absolute value. With kind permission from Springer Science + Business Media: T. K. Nayak, C. A. S. Regino, K. J. Wong, D. E. Milenic, K. Garmestani, K. E. Baidoo, L. P. Szajek and M. W. Brechbiel, *European Journal of Nuclear Medicine and Molecular Imaging*, **37**, 1368–1376. Fig. 3.[157]

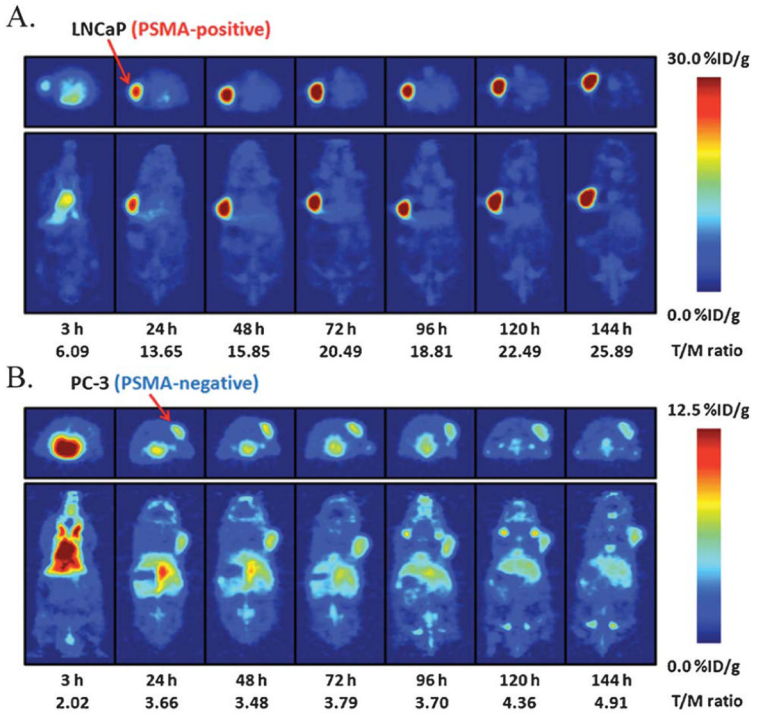

Fig. 9.

Temporal immunoPET images of ^{89}Zr-DFO-J591 recorded in (A) LNCaP tumor–bearing (PSMA-positive) and (B) PC-3 tumor–bearing (PSMA-negative) mice between 3 and 144 h after injection. Transverse and coronal planar images intersect the center of the tumors and the mean tumor-to-muscle ratios derived from volume-of-interest analysis of immunoPET images are given. Upper thresholds of immunoPET have been adjusted for visual clarity, as indicated by scale bars. Reprinted by permission of the Society of Nuclear Medicine from: J. P. Holland, V. Divilov, N. H. Bander, P. M. Smith-Jones, S. M. Larson and J. S. Lewis, *Journal of Nuclear Medicine*, 2010, **51**, 1293–1300. Fig. 4.[125]

Table 1

Physical decay characteristics of conventional PET radionuclides[158,159]

Radionuclide	Half-life	Decay mode (% branching ratio)	Production route	E(β^+)/keV	β^+ end-point energy/keV	Abundance, $I_{\beta+}$/%	E_γ/keV (intensity, I_γ/%)
^{11}C	1223.1 (12) s	β^+ (100)	^{14}N(p,a)^{11}C	385.6 (4)	960.2 (9)	99.759 (15)	511.0 (199.5)
^{13}N	9.965 (4) m	β^+ (100)	^{16}O(p,a)^{13}N	491.82 (12)	1198.5 (3)	99.8036 (20)	511.0 (199.6)
^{15}O	122.24 (16) s	β^+ (100)	^{15}N(p,n)^{15}O ^{14}N(d,n)^{15}O	735.28 (23)	1732.0 (5)	99.9003 (10)	511.0 (199.8)
^{18}F	109.77 (5) m	β^+ (100)	^{18}O(p,n)^{18}F ^{20}Ne(d,a)^{18}F	249.8 (3)	633.5 (6)	96.73 (4)	511.0 (193.5)
^{124}I	4.1760 (3) d	ε + β^+ (100) β^+ (22.7 [13])	^{124}Te(p,n)^{124}I	687.04 (85) 974.74 (85)	1,534.9 (19) 2,137.6 (19)	11.7 (10) 10.7 (9)	511.0 (45) 602.7 (62.9) 722.8 (10.4) 1,691.0 (11.2)

ε = electron capture; m = minutes; d = days; s = seconds. Where positrons or γ-rays of different energies are emitted, only those with abundances of greater than 10% are listed. Unless otherwise stated, standard deviations are given in parentheses.

Table 2

Physical decay characteristics of common PET radiometals[40]

Radionuclide	Half-life	Decay mode (% branching ratio)	Production route	E(β^+)/keV	β^+ end-point energy/keV	Abundance, $I_{\beta+}$/%	E_γ/keV (intensity, I_γ/%)	Ref.
^{64}Cu	12.701(2) h	ε + β^+ (61.5 [3]) β^+ (17.6 [22]) β^- (38.5 [3])	^{64}Ni(*p*,*n*)^{64}Cu	278.21 (9)	653.03 (20)	17.60 (22)	511.0 (35.2)	84, 85
^{68}Ga	67.71 (9) m	ε + β^+ (100) β^+ (89.14 [12])	^{68}Ge/^{68}Ga	836.02 (56)	1889.1 (12)	87.94 (12)	511.0 (178.3)	160, 70, 161
^{86}Y	14.74 (2) h	ε + β^+ (100) β^+ (31.9 [21])	^{86}Sr(*p*,*n*)^{86}Y	535 (7)	1221 (14)	11.9 (5)	443.1 (16.9) 511.0 (64) 627.7 (36.2) 703.3 (15) 777.4 (22.4) 1076.6 (82.5) 1153.0 (30.5) 1854.4 (17.2) 1920.7 (20.8)	77
^{89}Zr	78.4 (12) h	ε + β^+ (100) β^+ (22.74 [24])	^{89}Y(*p*,*n*)^{89}Zr	395.5 (11)	902 (3)	22.74 (24)	511.0 (45.5) 909.2 (99.0	79, 83, 162–164

ε = electron capture; m = minutes; h = hours; s = seconds. Where positrons or γ-rays of different energies are emitted, only those with abundances of greater than 10% are listed. Unless otherwise stated, standard deviations are given in parentheses.

Table 3

Coordination number, donor set, and geometry[a] for selected complexes of Cu(II), Ga(III), Y(III), and Zr(IV)[30]

Metal	Chelator	Ligand Donor Set	Total CN	Coordination Geometry	Ref.
Cu(II)	DTPA	N_3O_3	6	—	165
	NOTA	N_3O_3	6	distorted trigonal prism	166, 167
	DOTA	N_4O_2	6	distorted octahedron	168–170
	TETA	N_4O_2	6	distorted octahedron	168–170
	CB-TE2A	N_4O_2	6	distorted octahedron	101, 171
	EC	N_2S_2	4	distorted square planar	172
	DIAMSAR	N_6	6	distorted octahedron or trigonal prism	173
Ga(III)	EDTA	N_2O_4	6	distorted octahedron	174, 175
	HBED	N_2O_4	6	—	176, 177
	DTPA	N_3O_3	6?	—	175
	NOTA	N_3O_3	6	distorted octahedron	168, 178
	DOTA	N_4O_2	6	distorted octahedron	168
	TETA	N_4O_2	6	distorted octahedron	168
	CB-TE2A	N_4O_2	6	distorted octahedron	30, 179
	DFO	O_6	6	—	180
Y(III)	DTPA	N_3O_5	8	monocapped square antiprism	116, 181, 182
	DOTA	N_4O_4	8	square antiprism	114, 116, 182
	TETA	N_4O_2	8?	distorted dodecahedron(?)	183
Zr(IV)	DFO	O_6	7 or 8	—	125
	DOTA	N_4O_4	8?	square antiprism?	115
	EDTA	N_2O_4	8	distorted dodecahedron	181, 184
	DTPA	N_3O_5	8	distorted dodecahedron	181, 184

[a]Question marks denote uncertainty in coordination number or geometry, and "—" denotes that the coordination geometry is not known.

Table 4

Guide to the construction of ^{68}Ga-peptide bioconjugates

Chelator	Target	Conjugation	Radiometallation[a]	Purification
DOTA	VAP-1[185]	Peptide was coupled on the bead to DOTA(tBu)$_3$ using an automated peptide synthesizer. Removal of the peptide from the support, deprotection, and RP-HPLC followed.	^{68}Ga eluent was adjusted to pH 5.5 with NaOAc, followed by addition of the peptide and incubation for 10–20 min at 90–100 °C.	None reported
	EGFR[127]	Peptide in borate buffer (0.08 M, pH 9.4) was added to dry DOTA-NHS. The pH of the resultant solution was adjusted to 9.0 with additional borate, and the mixture was allowed to stir overnight at RT, followed by RP-HPLC.	Peptide was incubated with ^{68}Ga for 1 min at 90 °C *via* microwave in either NaOAc (pH 5.0, for use with non-concentrated eluent) or HEPES (pH 4.7, for use with concentrated eluent).	C_{18} cartridge
	GRPR[128,186]	Peptide on resin was mixed with a pre-incubated solution of DOTA(tBu)$_3$ and HATU in *N*-methylpyrrolidone (adjusted to pH 7–8 using DIPEA), followed by cleavage from resin, deprotection, and purification.	^{68}Ga eluent was dried and redissolved in NaOAc (0.1 M, pH 4.8), followed by addition of the peptide and incubation for 10 min at 90 °C.	C_{18} cartridge
	NTR[187]	Peptide was coupled on the bead to DOTA(tBu)$_3$ using an automated peptide synthesizer. Removal of the peptide from the support, deprotection, and purification followed.	Peptide was incubated with ^{68}Ga in NaOAc (concentration not noted, pH 4.5) for 10 min at 95 °C.	None reported
	SSTR[126,188,189] GRPR[126]	Peptide was coupled on the bead to DOTA(tBu)$_3$ using an automated peptide synthesizer. Removal of the peptide from the support, deprotection, and purification followed.	^{68}Ga eluent was adjusted to pH 3.5–3.8 with 1 M HEPES and incubated with the peptide for 4 min at 90 °C.	C_{18} cartridge
	GRPR[190,191]	Peptide was coupled on the bead to DOTA(tBu)$_3$ with HATU using an automated peptide synthesizer. Removal of the peptide from the support, deprotection, and purification followed.	^{68}Ga eluent was dried and redissolved in NaOAc (0.1 M, pH 4.8), followed by addition of peptide and incubation for 10 min at 90 °C.	C_{18} cartridge
	MC1-R[192,193]	Deprotected peptide was dissolved in DMF with DIEA (1.5%) and added to a solution of DOTA(tBu)$_3$ and HATU, which had beenincubated in DMF for 10 min at RT. The resultant solution was stirred at RT for 1 h, followed by precipitation, deprotection, and RP-HPLC.	Peptide was incubated with ^{68}Ga in NaOAc (0.1 M, pH 4.8) for 15 min at 90 °C.	C_{18} cartridge
	SSTR[132,133]	DOTA(tBu)$_3$, HATU, and DIEA (1 : 1 : 1) were incubated with DMF for 10 min at RT, followed by addition of the peptide (in DMF with 1.5% DIEA) and stirring for 4 h at RT. Extraction, deprotection, and RP-HPLC followed.	Peptide was incubated with ^{68}Ga in NaOAc (0.4 M, pH 4.8–5.5) for 15–25 min at 95 °C.	C_{18} cartridge
	SSTR[134]	Conjugate was purchased from a commercial supplier.	Peptide was incubated with ^{68}Ga in NaOAc (0.1 M, pH 4.5) for 5 min at 95 °C.	C_{18} cartridge
	SSTR[135]	Conjugate was purchased from a commercial supplier.	^{68}Ga eluent in 0.05 M HCl/acetone (2 : 98) was added	C_{18} cartridge

Chelator	Target	Conjugation	Radiometallation[a]	Purification
			directly to the peptide in water and incubated for 10 min at 100 °C.	
	SSTR[148]	Hydroxylamine-modified peptide was incubated with deprotected acetyl-Bn-DOTA in 1 : 1 CH_3CN : H_2O (adjusted to pH 4 with TFA) for 18 h at RT, followed by RP-HPLC.	Experimental details were not given, though radiometallation was reported in publication.	None noted
HBED	VEGFR[194]	**1** Formation of the activated ester of Fe(HBED-CC) complex with NHS and EDC in DMF–H_2O **2** Reaction of Fe-HBED-CC-NHS with NH_2-PEG-maleimide in MES buffer (0.5 M, pH 8.0) for 30 min at RT, followed by RP cartridge (1 M HCl) to remove Fe^{3+} **3** Reaction of HBED-CC-PEG-maleimide with deprotected peptide in carbonate buffer (pH 8.0) for 1 h **4** Purification *via* C_4 RP-HPLC	Peptide solution (0.1 M phosphate buffer, pH 7.0) was combined with 10 μL ^{68}Ga solution and 10 μL 2.1 M HEPES, for a final pH of 4.2. Time and temperature were not noted.	Size exclusion chromatography
NOTA	VEGFR[194,195]	Peptide modified with NHS-PEG group was incubated with *p*-NH_2-Bn-NOTA in carbonate buffer (pH 8.0) for 1 h, followed by C_4 RP-HPLC.	Same as above	Size exclusion chromatography
	$\alpha_v\beta_3$[129,196] GRPR[196]	Peptide was incubated with *p*-SCN-Bn-NOTA in $NaHCO_3$ (0.1 M, pH 9.0) for 5 h at RT, followed by RP-HPLC.	Peptide was incubated with ^{68}Ga in NaOAc (0.1 M, pH 5) for 10–15 min at 40–45 °C.	RP-HPLC
	$\alpha_v\beta_3$[197]	Peptide was incubated with *p*-SCN-Bn-NOTA in $NaHCO_3$ (0.1 M, pH 9.5) for 20 h at RT, followed by RP-HPLC.	^{68}Ga eluent was adjusted to pH 6.0 with 7% $NaHCO_3$ solution, followed by addition of peptide for 10 min at RT.	RP-HPLC
	SSTR[131]	Peptide on resin was mixed with a pre-incubated solution of $NODAGA(tBu)_3$ and HATU in *N*-methylpyrrolidone (adjusted to pH 7–8 using DIPEA), followed by cleavage from resin, deprotection, and RP-HPLC.	Peptide was incubated with ^{68}Ga in NaOAc (0.4 M, pH 5) or HEPES (0.1 M, pH 5.8) for 25 min at 95 °C	C_{18} cartridge
DFO	SSTR[198]	Peptide bearing an activated succinimidyl ester was incubated with DFO mesylate in DMF with DCC/HOBT. Time, temperature, and intermediate purification were not noted.	Peptide (in 0.1% AcOH) was incubated with ^{68}Ga (in 0.1 M NH_4OAc, pH 4.5) for 5 min at RT.	None reported
DTPA	LDL[199,200]	Peptide was reacted with cyclic DTPA anhydride in HEPES buffer (0.1 M, pH 7) for 30 min at RT, followed by size exclusion chromatography. Other buffer types	^{68}Ga eluent was dried and re-dissolved in NaOAc (0.4 M, pH 7.0), followed by addition of peptide and	Size exclusion chromatography

Chelator	Target	Conjugation	Radiometallation[a]	Purification
		were reported to work for this reaction as well.	incubation for 1–30 min at RT.	
	None (HSA)[201]	Peptide was incubated with mixed acid anhydride DTPA in aqueous buffer (type and concentration not noted) for 12 h at 4 °C, followed by size exclusion chromatography.	DTPA-HSA solution pH was lowered to 3.1 with 1 M HCl, followed by addition of ^{68}Ga solution (in 1 : 3 EtOH:0.9% NaCl), incubation at RT for 30 min, and final adjustment of pH to 5.5 with 0.1 M NaOH.	Size exclusion chromatography

[a]Some protocols call for the use of gentisic acid (typically 1–5 mg mL^{-1}) to protect the biomolecule from radiolysis.

Table 5

Guide to the construction of ^{68}Ga-antibody bioconjugates

Chelator	Target	Conjugation	Radiometallation[a]	Purification
HBED	EGFR[112] EpCAM[112,202]	**1** Synthesis of Fe(HBED-CC) **2** Formation of an activated ester of the Fe(HBED-CC) complex *via* reaction with TFP and DCC in DMF for 2 d at RT, followed by HPLC purification and removal of Fe^{3+} with RP-cartridge using 1 M HCl **3** Incubation of HBED-CC-TFP (from DMSO stock) with antibody fragment in carbonate/phosphate buffer (pH 8) for 30 min at RT, followed by size exclusion chromatography.	Antibody solution (0.1 M phosphate buffer, pH 7.0) was combined with ^{68}Ga eluent and 2.1 M HEPES (for a final pH of 4.1–4.5) and incubated for 5–10 min at RT (40 °C).	Size exclusion chromatography
DOTA	HER2[203–205]	Active DOTA ester was first formed *via* reaction of DOTA with NHS and subsequently EDC at RT, followed by cooling to 4 °C for 1 h and incubation with antibody fragment solution (0.1 M sodium phosphate, pH 7.0) overnight at 4 °C. Excess DOTA was removed with centrifugal filtration.	Antibody solution (in 1 M NH_4OAc stock) was combined with ^{68}Ga eluent (in 0.1 M HCl) and incubated for 15 min at 37 °C. Final reaction pH was not noted.	Size exclusion chromatography
	HER2[206–208]	Affibody was synthesized using standard solid phase synthesis and Fmoc chemistry, followed by conjugation on the bead with $DOTA(tBu)_3$-NHS and subsequent deprotection, removal from the bead, and purification.	^{68}Ga eluent (in 0.1 M HCl) was combined (~1 : 1) with affibody in NH_4OAc (1.25 M, pH 4.2) and incubated for 10 min at 90 °C.	None noted
DTPA	hPSP[209,210]	Antibody was incubated with DTPA cyclic anhydride in aqueous solution (buffer conditions not described), followed by size exclusion chromatography to remove excess DTPA.	^{68}Ga eluent was evaporated to dryness, reconstituted in NH_4OAc buffer (0.1 M), and incubated with antibody. Time, pH, and temperature were not noted.	Size exclusion chromatography
DTPA	CD45[211]	Antibody was incubated with *p*-SCN-DTPA, mx-DTPA, or CHX-A″-DTPA in HEPES buffer (0.05 M, pH 9.5) for 20 h at RT, followed by size exclusion chromatography.	^{68}Ga eluent pH was adjusted to ~5 with 1 M NaOAc, followed by addition of antibody for 10 min at RT. Reaction was quenched with DTPA.	Size exclusion chromatography

[a] Some protocols call for the use of gentisic acid (typically 1–5 mg mL^{-1}) to protect the biomolecule from radiolysis.

Table 6

Guide to the construction of radiometallated oligonucleotide bioconjugates

Chelator	Nuclide	Type	Conjugation	Radiometallation	Purification
DOTA	^{86}Y	RNA oligomer[120]	Amine-modified oligomer was incubated with *p*-SCN-Bn-DOTA in $NaHCO_3$ buffer (0.7 M, pH 9.0) for 2 h at 40 °C, followed by purification *via* EtOH precipitation and size exclusion chromatography.	Oligomer was incubated with ^{86}Y in NH_4OAc buffer (0.5 M, pH 7.0) for 30–60 min at 90 °C. Reaction quenched with DTPA.	RP-HPLC
	^{86}Y	RNA oligomer[138]	Amine-modified oligomer was incubated with DOTA-NHS in $NaHCO_3$ buffer (0.7 M, pH 8.1) for 2 h at 40 °C, followed by purification *via* size exclusion chromatography.	Oligomer was incubated with ^{86}Y in NH_4OAc buffer (0.5 M, pH 6.0) for 45 min at 90 °C. Reaction quenched with DTPA.	C_{18} cartridge
	^{64}Cu	PNA-peptide conjugate[55,212]	Amine-modified PNA/peptide conjugate on a solid support was reacted with $DOTA(tBu)_3$ and HATU on a peptide synthesizer for 60 min, followed by cleavage, deprotection, and RP-HPLC.	Conjugate was incubated with ^{64}Cu in NH_4OAc buffer (0.1 M, pH 5.5) for 15 min at 90 °C.	RP-HPLC
	^{64}Cu	PNA[213]	$DOTA(tBu)_3$ (in N-methylpyrrolidone) was combined with HATU (in DMF) and base (DIEA and 2,6-lutidine in DMF) and subsequently manually reacted with resin-bound PNA for 1 h at RT, followed by cleavage, deprotection, and RP-HPLC.	$^{64}CuCl_2$ was converted to ^{64}Cu-citrate with NH_4-citrate (0.1 M, pH 7.0) and incubated with PNA in buffer for 1–2 h at 60 °C. Reaction quenched with DTPA.	Centrifugal column filtration
	^{68}Ga	RNA oligomer[138]	Amine-modified oligomer was incubated with DOTA-NHS in $NaHCO_3$ buffer (0.7 M, pH 8.1) for 2 h at 40 °C, followed by purification *via* size exclusion chromatography.	Oligomer was incubated with ^{68}Ga in NH_4OAc buffer (0.5 M, pH 4.1–4.7) for 45 min at 90 °C. Reaction quenched with DTPA.	C_{18} cartridge
	^{68}Ga	DNA, PS, and OMe oligomers[137,214]	Activated ester was formed *via* the incubation of DOTA with SNHS and EDC in H_2O from 4 °C to RT over 30 min. This mixture was added to amine-modified oligonucleotide solution in carbonate buffer (1 M, pH 9) overnight at 4 °C, followed by purification *via* size exclusion chromatography and C_{18} cartridge.	^{68}Ga eluent was adjusted to pH 5.5 with NaOAc, followed by addition of oligonucleotide for 10 min at 100 °C.	C_{18} cartridge
	^{68}Ga	DNA-LNA oligomer[136,214]	Amine modified oligomer was incubated with DOTA-SNHS in $Na_2B_4O_7$ buffer (adjusted to pH 8.5–10 with 5 M NaOH) overnight at 4 °C, followed by purification by centrifugal column filtration.	Oligomer was added to purified ^{68}Ga eluent (HEPES, pH 4.6–5.0) and heated to 90 °C for 1 min in a microwave.	C_4 cartridge
$SBTG_2DAP$	^{64}Cu	PNA-peptide conjugate[215]	Using an automated peptide synthesizer, diaminopropanoate-modified PNA/peptide conjugate on a solid support was reacted with two equivalents of S-benzoyl thioglycolic acid using HATU and *N*-methylmorpholine in DMF.	Conjugate was incubated with ^{64}Cu in NH_4OAc buffer (0.1 M, pH 5.5) for 30 min at 90 °C.	RP-HPLC

Table 7

Guide to the construction of ^{64}Cu-peptide bioconjugates

Chelator	Target	Conjugation[a]	Radiometallation[b,c]
DOTA	GRPR[156,216,217] SSTR[218]	Peptide was coupled to DOTA(tBu)$_3$ or DOTA(tBu)$_3$-NHS using an automated peptide synthesizer and standard Fmoc chemistry, followed by cleavage from the resin, deprotection, and purification.	Peptide was incubated with ^{64}Cu in NH_4OAc (0.1 M, pH 5.5) for 30 min at RT.
	MC1-R[219,220]	Peptide was coupled to DOTA(tBu)$_3$ using an automated peptide synthesizer and standard Fmoc chemistry, followed by cleavage from the resin, deprotection, and purification.	Peptide was incubated with ^{64}Cu in NaOAc (0.1 M, pH 5.5) for 60 min at 65 °C.
	GRPR[221]	Peptide was coupled to DOTA(tBu)$_3$ while still on the peptide synthesizer, followed by cleavage from resin, deprotection, and purification.	Peptide was incubated with ^{64}Cu in NH_4OAc (0.4 M, pH 7) for 40 min at 70 °C.
	$\alpha_v\beta_6$[222]	Peptide was coupled to DOTA(tBu)$_3$ using HATU/DIEA while peptide was still on the resin, followed by cleavage from the resin, deprotection, and purification.	Peptide was incubated with ^{64}Cu in NH_4OAc (1 M, pH 7–8) for 60 min at RT. Reaction quenched with EDTA.
	GRPR[223]	The method of DOTA incorporation method is unclear; however, a tributyl anhydride of DTPA was used for the acylation of prolines in similar DTPA-modified conjugates, so a similar strategy may have been used here.	Peptide was incubated with ^{64}Cu in NH_4OAc (0.5 M, pH 6.5) for 30 min at 80 °C.
	$\alpha_v\beta_3$[224–228] GRPR[229] VEGFR[230,231] UPar[232] IL-18R[233,c]	DOTA was activated for coupling *via* reaction with EDC and *N*-hydroxysulfosuccinimide (SNHS) (10 : 5 : 4) in water (pH 5.5) for 30 min at 4 °C. Peptide (in water, buffer, or saline) was then added to the solution, the pH was adjusted to 8.5 with 0.1 M NaOH, and the resultant solution was stirred for 16 h at 4 °C.	Peptide was incubated with ^{64}Cu in NaOAc (0.1 M, pH 5–6.5) for 30–60 min at 40–50 °C. In some cases the reaction was quenched with EDTA.
	MC1-R[234,235] $\alpha_v\beta_3$[235,c]	DOTA was activated for coupling *via* reaction with EDC and SNHS (1 : 1 : 0.8) in water (pH 5.5) for 30 min at 4 °C. Peptide (in phosphate buffer or water) was then added to the solution, the pH was adjusted to 8.5–9.0 with 0.1 M NaOH, and the resultant solution was stirred for 16 h at 4 °C.	Peptide was incubated with ^{64}Cu in NaOAc (0.1 M, pH 5.5) for 60 min at 37–50 °C.
	$\alpha_v\beta_3$[236]	DOTA was initially activated for coupling *via* 1 : 1 : 1 reaction with SNHS and EDC in water (pH 5.5) for 40 min at RT. Peptide in phosphate buffer (30 mM, pH 8.5) was then added to the solution, the pH was adjusted to 8.5 with 0.1 M NaOH, and the resultant solution was stirred for 1 h at RT and then 16 h at 4 °C.	Peptide was incubated with ^{64}Cu in NaOAc (0.1 M, pH 6.3) for 60 min at 45 °C.[c]
	$\alpha_v\beta_3$[224]	Peptide was incubated with (tBu)$_3$ DOTA, HBTU, and Hunig's Base in DMF overnight at RT, followed by deprotection, and purification.	Peptide was incubated with ^{64}Cu in NaOAc (0.5 M, pH 5.5) for 45 min at 50 °C.
	NPR[237,238]	Peptide was incubated with DOTA-NHS overnight in Na_2HPO_4 buffer (0.1 M, pH 7.5) at RT.	Peptide was incubated with ^{64}Cu in NH_4OAc (0.1 M, pH 5.5) for 60 min at 43 °C.
	GC-C[239]	Peptide was incubated with DOTA-NHS in HEPES buffer (0.3 M, pH 8.5) overnight at 4 °C.	Peptide was incubated with ^{64}Cu in NH_4OAc (0.4 M, pH 6.0) for 1 h at 80 °C. Reaction quenched with EDTA.
	FPR[240]	Peptide was incubated with DOTA-NHS in water (pH 8.5) overnight at 4 °C.	Peptide was incubated with ^{64}Cu in NH_4OAc (0.1 M, pH 5.5) for 30 min at 40 °C.
	VEGFR[195,241]	*p*-NH_2-Bn-DOTA was activated *via* reaction with NHS-PEG-maleimide in buffer (15 mM NaOAc,	Peptide was incubated with ^{64}Cu in NaOAc (0.1 M, pH 5.3–5.5) for 60

Chelator	Target	Conjugation[a]	Radiometallation[b,c]
		50 mM Na_2CO_3, 115 mM NaCl, pH 8.0) at RT for 1 h, followed by quenching of excess maleimide with Tris HCl (1 M, pH 8.0), the addition of peptide, incubation for 1 h at RT, and RP-HPLC with a C_4 column.[d]	min at 55 °C. Reaction quenched with EDTA.[d]
	Low pH[242]	Peptide was incubated with DOTA-maleimide in PBS (pH 7, with 2 mM EDTA) overnight at 4 °C.[d]	Peptide was incubated with ^{64}Cu in NH_4OAc (0.5 M, pH 5.5) for 30 min at RT. Reaction quenched with EDTA.
CB-TE2A	MC1-R[243]	Peptide was coupled to CB-TE2A using standard Fmoc/HBTU chemistry on a peptide synthesizer, followed by cleavage from the resin and deprotection.	Peptide was incubated with ^{64}Cu in NH_4OAc (0.1 M, pH 8) for 60 min at 95 °C.
	SSTR[244]	Peptide was reacted while still on the resin with CB-TE2A that had been pre-activated with DIEA and DCC, followed by cleavage from the resin, deprotection, and purification.	Peptide was incubated with ^{64}Cu in NH_4OAc (0.1 M, pH 8) for 90 min at 95 °C.
	SSTR[50,245]	CB-TE2A was dissolved in DMF with DIEA and DIC and stirred for 25 min at RT before adding the solution to the peptide-containing resin. The resultant mixture was agitated for 3 h before filtration, washing, cleavage, and purification.	Peptide was incubated with ^{64}Cu in NH_4OAc (0.1 M, pH 8) for 60–90 min at 95 °C.
	$\alpha_4\beta_1$[246]	CB-TE2A was dissolved in DMF with DIEA and DIC and stirred for 25 min at RT before adding the solution to the peptide-containing resin. The resultant mixture was agitated overnight before filtration, washing, cleavage, and purification.	Peptide was incubated with ^{64}Cu in NH_4OAc (0.14 M, pH 7) for 60 min at 95 °C.
	GRPR[221]	Peptide was coupled to CB-TE2A precursor on peptide synthesizer, followed by cleavage from resin, deprotection, and purification.	Peptide was incubated with ^{64}Cu in NH_4OAc (0.4 M, pH 7) for 40 min at 70 °C.
	$\alpha_v\beta_6$[222]	CB-TE2A was pre-activated with DIC in DIEA and subsequently reacted with resin-bound peptide for 30 min at RT, followed by cleavage from the resin, deprotection, and purification.	Peptide was incubated with ^{64}Cu in NH_4OAc (1 M, pH 7.5–8.5) for 60 min at 95 °C. Reaction quenched with EDTA.
	$\alpha_v\beta_3$[99,247,248]	Peptide was reacted with CB-TE2A in the presence of DIC and HOBT in anhydrous DMF, followed by deprotection and purification.	Peptide was incubated with ^{64}Cu in NH_4OAc (0.1 M, pH 8) for 45–120 min at 95 °C.
TETA	SSTR[249,250]	Lys-protected peptide was conjugated *in situ* to TETA *via* reaction with DIEA, DIC/HOBT, and HBTU in DMF (time and temperature not noted), followed by deprotection and purification.	Peptide incubated with ^{64}Cu in NH_4OAc (0.1 M, pH 5.5) for 30 min at RT.
	SSTR[50]	Peptide was coupled to TETA$(tBu)_3$ using standard Fmoc chemistry on an automated peptide synthesizer.	Peptide was incubated with ^{64}Cu in NH_4OAc (0.1 M, pH 5.5) for 1 h at RT.
	SSTR[245,251–253]	Peptide was coupled to TETA$(tBu)_3$ using standard Fmoc chemistry on an automated peptide synthesizer.	Peptide was incubated with ^{64}Cu in NH_4OAc (0.1 M, pH 5.5–6.5) for 1 h at RT-37 °C.
	GC-C[239]	The activated ester of TETA was formed with EDC and SNHS in sodium phosphate buffer (0.2 M, pH 8.0), followed by the addition of peptide and incubation overnight at 4 °C.	Peptide was incubated with ^{64}Cu in NH_4OAc (0.4 M, pH 6.0) for 1 h at 80 °C. Reaction quenched with EDTA.
	$\alpha_3\beta_1$[99,254]	Resin-bound peptide was combined with HBTU, DIEA, and TETA (from DMSO stock) and stirred for 4 h at RT, followed by cleavage from resin and deprotection.	Peptide was incubated with ^{64}Cu in NH_4OAc (0.1 M, pH 5.5, 1% BSA) for 15–30 min at RT. Reaction quenched with EDTA.
NOTA	GRPR[255,256]	NOTA was activated for coupling *via* reaction with SNHS and EDC in MES buffer (0.1 M, pH 4.7) for 10 min at RT. Peptide (in phosphate buffer, pH 7.4) was then added to the solution, the	Peptide was incubated with ^{64}Cu in NH_4OAc (0.4 M, pH 7.0) for 1 h at

Chelator	Target	Conjugation[a]	Radiometallation[b,c]
		pH was adjusted to 7.4 with 10% NaOH, and the resultant solution was stirred for 16 h at RT.	70 °C. Reaction quenched with DTPA.
	GC-C[239]	The activated ester of NOTA was formed with EDC and SNHS in sodium phosphate buffer (0.2 M, pH 8.0), followed by the addition of peptide and incubation overnight at 4 °C.	Peptide was incubated with ^{64}Cu in NH_4OAc (0.4 M, pH 6.0) for 1 h at 80 °C. Reaction quenched with EDTA.
	GRPR[196] $\alpha_v\beta_3$[196]	Peptide was incubated with *p*-SCN-Bn-NOTA in $NaHCO_3$ buffer (0.1 M, pH 9.0) for 5 h at RT.	Peptide was incubated with ^{64}Cu in NaOAc (0.1 M, pH 6.5) for 15 min at 40 °C.
CPTA	SSTR[249]	Lys-protected peptide was conjugated *in situ* to CPTA *via* reaction with DIC and HOBT in DMF (time and temperature were not noted), followed by deprotection and purification.	Peptide was incubated with ^{64}Cu in NH_4OAc (0.1 M, pH 5.5). Time and temperature were not noted.
Bis(2-mercaptoacetamide)	VPAC[257,258]	Protected chelator precursors were incorporated into the peptide *via* automated, solid-phase peptide synthesis using standard Fmoc/DIC/HOBT chemistry.	Peptide was incubated with ^{64}Cu in glycine buffer (0.2 M, pH 9), $SnCl_2{\cdot}2H_2O$ (0.1 M), and HCl (0.05 M) for 20–45 min at 90 °C.
BPM-TACN	GRPR[259]	Peptide was dissolved in DMF with chelator and HBTU. Subsequently, DIPEA was added, and the resultant solution was stirred for 20 h at RT.	^{64}Cu in NH_4OAc (0.1 M) was added to peptide in 1 : 1 MeCN : H_2O and incubated for 30 min at 40 °C.
DiamSar	$\alpha_v\beta_3$[247]	Peptide was reacted with DiamSar in the presence of DIC and HOBT in anhydrous DMF, followed by deprotection.	Peptide was incubated with ^{64}Cu in NH_4OAc (0.1 M, pH 8.0) for 1 h at RT.
AmBaSar	$\alpha_v\beta_3$[260]	AmBaSar was activated for coupling *via* reaction with EDC and SNHS (1 : 1 : 0.8) in water (pH 5.5) for 30 min at 4 °C. Peptide (in water) was then added to the solution, the pH was adjusted to 8.6 with 0.1 M NaOH, and the resultant solution was stirred for 16 h at RT.	Peptide was incubated with ^{64}Cu in NH_4OAc (0.1 M, pH 5.0) for 60 min at RT.
	$\alpha_v\beta_3$[261]	AmBaSar, HATU, HOAt, and DMSO were stirred at RT for 10 min, followed by the addition of DIPEA and peptide to the solution at 0 °C and incubation for 3 h at RT.	Peptide was incubated with ^{64}Cu in NH_4OAc (0.1 M, pH 5.0) for 30 min at RT.

[a] Unless otherwise noted, peptide-chelator constructs were purified with RP-HPLC or C_{18} cartridge prior to radiolabeling.

[b] Unless otherwise noted, final radiometallated peptides were purified by RP-HPLC or C_{18} cartridge.

[c] Some protocols call for the use of gentisic acid (typically 1–5 mg mL^{-1}) to protect the biomolecule from radiolysis.

[d] Purified *via* size exclusion chromatography

Table 8

Guide to the construction of ^{64}Cu-antibody bioconjugates

Chelator	Target	Conjugation	Radiometallation[a]	Purification
DOTA	HER2[262]	Reduced affibody (in PBS, pH 7.4) was incubated with maleimide-modified DOTA (from a stock in DMSO) for 2 h at RT, followed by purification *via* overnight dialysis.	Affibody was incubated with ^{64}Cu in NaOAc (0.1 M, pH 5.5) for 1 h at 40 °C.	Size exclusion chromatography
	HER2[263,264] CEA[264]	Activated DOTA was prepared *via* the combination of DOTA, SNHS and EDC (1 : 1 : 0.1) in water (pH 5.5) for 30 min at 4 °C. This solution was then adjusted to pH 7.3 with Na_2HPO_4 (0.2 M, pH 9.2), added to antibody (in NaH_2PO_4, 0.1 M, pH 7.5), and incubated overnight at 4 °C. Centrifugal column filtration followed.	Antibody was incubated with ^{64}Cu in NH_4-citrate (0.1 M, pH 5.5) for 50–60 min at 43 °C. Reaction quenched with EDTA.	Size exclusion chromatography
	$\alpha_v\beta_3$[51] EGFR[53,265,266]	Activated DOTA was prepared *via* the combination of DOTA, EDC, and SNHS (10 : 5 : 4) in water (pH 5.5) for 30 min at RT. This solution was then added to antibody, the pH of the reaction mixture was adjusted to 8.5 with 0.1 M NaOH, and the solution was incubated overnight at 4 °C. Size exclusion chromatography followed for purification.	Antibody was incubated with ^{64}Cu in NaOAc (0.1 M, pH 6.5) for 1 h at 40 °C.	Size exclusion chromatography
	HER2[267]	Antibody was incubated with DOTA-NHS (from DMSO stock) in borate-buffered saline (0.1 M pH 8.5) for 16 h at RT, followed by size exclusion chromatography.	Antibody was incubated with ^{64}Cu in NaOAc (0.25 M, pH 6.0) for 1.5 h at 40 °C. Reaction quenched with EDTA.	Size exclusion chromatography
	CEA[268] TAG-72[269]	Antibody was first dialyzed against PBS (pH 7.2) and $NaHCO_3$ (0.1 M, pH 8.5). DOTA-NHS was then added to the antibody solution and incubated for 2 h at RT, followed by dialysis for purification.	Antibody was incubated with ^{64}Cu in NH_4-citrate (0.1 M, pH 5.5) for 45 min at 43 °C.	Size exclusion chromatography
	CD22[270]	Antibody was incubated with DOTA-NHS in tetramethyl ammonium phosphate (0.1 M, pH 8) for 2.5 h at 37 °C, followed by centrifugal column filtration.	Antibody was incubated with ^{64}Cu in NH_4OAc (0.25 M, pH 7) for 1 h at 40 °C. Reaction quenched with EDTA.	Centrifugal column filtration
	PSMA[271]	Antibody was incubated with DOTA-NHS in Na_2HPO_4 (0.1 M, pH 7.5) for 24 h at 4 °C, followed by dialysis for purification.	Antibody was incubated with ^{64}Cu in NH_4OAc (0.25 M, final pH 5.5) for 40 min at 40 °C. Reaction quenched with DTPA.	None listed
	EGFR[272]	Antibody was incubated with $(tBu)_3$ DOTA-NHS in Na_2HPO_4 buffer (0.1 M, pH 7.4) for 16 h at 4 °C, followed by centrifugal column filtration.	Antibody was incubated with ^{64}Cu in NH_4-citrate (0.1 M, pH 5.5) for 1 h at 40 °C.	Size exclusion chromatography
	L1-CAM[273]	Antibody in phosphate buffer (0.1 M, pH 8) was added to DOTA-NCS variants. The pH was adjusted to 9–10 with Na_3PO_4, and the solution was incubated for 16 h at 4 °C, followed by centrifugal column filtration.	Antibody was incubated with ^{64}Cu in NaOAc (0.1 M, pH 5.5) for 1 h at RT. Reaction quenched with EDTA.	Size exclusion chromatography
CPTA	L1-CAM[273,274]	Antibody was incubated with CPTA-NHS in sodium phosphate buffer (0.1 M, pH 7) for 2 h at RT, followed by centrifugal column filtration.	Antibody was incubated with ^{64}Cu in NaOAc (0.1 M, pH 5.5) for 1 h at RT. Reaction quenched with EDTA.	Size exclusion chromatography
DO3A	L1-CAM[273]	Antibody in phosphate buffer (0.1 M, pH 8) was added to DO3A-Bn-NCS. The pH was adjusted to 9–10 with Na_3PO_4, and the	Antibody was incubated with ^{64}Cu in NaOAc (0.1 M, pH 5.5) for 1 h at RT.	Size exclusion chromatography

Chelator	Target	Conjugation	Radiometallation[a]	Purification
		solution was incubated for 16 h at 4 °C, followed by centrifugal column filtration.	Reaction quenched with EDTA.	
	CEA[268]	**1** Generation of sulfhydryls on antibody *via* incubation with SATA[b] followed by $NH_2OH{\cdot}HCl$ **2** Purification *via* size exclusion chromatography **3** Incubation with DO3A-VS in PBS for 2 h at RT **4** Purification *via* dialysis	Antibody was incubated with ^{64}Cu in NH_4-citrate (0.1 M, pH 5.5) for 45 min at 43 °C.	Size exclusion chromatography
	CEA[268]	Antibody was incubated DO3A-VS in PBS (adjusted to pH 9.0 with 0.1 M NaOH) for 18 h at RT, followed by dialysis.	Antibody was incubated with ^{64}Cu in NH_4-citrate (0.1 M, pH 5.5) for 45 min at 43 °C.	Size exclusion chromatography
TETA	CC[17,275]	Antibody in ammonium phosphate (0.1 M, pH 8.0) was incubated with excess Br-benzyl-TETA and fresh 2-iminothiolane in triethanolamine (50 mM) for 30 min at 37 °C, followed by centrifugal column filtration.	Antibody was incubated with ^{64}Cu in NH_4-citrate (0.1 M, pH 5.5) for 15–30 min at RT.	Size exclusion chromatography
SarAr	GD2[54]	Antibody was incubated with SarAr and EDC in NaOAc (0.1 M, pH 5.0) for 30 min at 37 °C, followed by size exclusion HPLC.	Antibody was incubated with ^{64}Cu in NaOAc (0.1 M, pH 5.0) for 30 min at 37 °C.	None reported

[a] Some protocols call for the use of gentisic acid (typically 1–5 mg mL^{-1}) to protect the biomolecule from radiolysis.

[b] SATA = S-acetylthioacetate

Table 9

Guide to the construction of ^{86}Y bioconjugates

Chelator	Target	Vector	Conjugation	Radiometallation[a]	Purification
CHX-A″-DTPA	EGFR[157,276] HER1[277,278]	Antibody	Antibody (in 0.05 M bicarbonate buffer and 0.001 M EDTA, pH 8.0) was incubated with CHX-A″-DTPA (from stock in same buffer) for 4 h at 37 °C, followed by removal of the unbound chelate by dialysis against 0.15 M NH_4OAc.	^{86}Y solution (in 0.1 M nitric acid) was adjusted to pH 5–6 with NH_4OAc buffer (5 M, pH 7.0), followed by addition of antibody (in 0.15 M NH_4OAc) and incubation for 30 min at RT. Reaction quenched with EDTA.	Size exclusion chromatography
	Lewis Y antigen[279–281]	Antibody and antibody fragments	Antibody was dialyzed against sodium bicarbonate buffer (0.05 M, pH 8.6) containing 0.15 M NaCl for 6 h. CHX-A″-DTPA was added to the mAb solution and incubated at RT overnight in the dark. Unbound chelate was removed by dialysis for 8 h against 20 mM NH_4OAc with 0.15 M NaCl (pH 6.3).	^{86}Y-acetate was prepared by mixing stock ^{86}Y solution with NH_4OAc (3 M, final pH 5.0), followed by addition of antibody and incubation for 30 min at RT. Reaction quenched with EDTA.	Size exclusion chromatography
	Mindin/RG1[282]	Antibody	Antibody (in 0.05 M sodium bicarbonate, 0.15 M NaCl, pH 8.5) was incubated with CHX-A″-DTPA (from DMSO stock) overnight at RT, followed by size exclusion chromatography.	^{86}Y solution (0.1 M HCl) was diluted three-fold with NH_4OAc (0.1 M, pH 5.6) and subsequently added to antibody for incubation at RT for 1 h. Reaction quenched with EDTA.	Size exclusion chromatography
	MC1-R[283]	Peptide	Peptide was incubated with NHS ester of CHX-A″-DTPA glutarate ligand in DMF in the presence DIEA for 2 h at RT, followed by diethyl ether precipitation, deprotection, and RP-HPLC purification.	^{86}Y (in 0.1 M HCl) was incubated with peptide (in 0.5 M NH_4OAc, pH 5.5) at 75 °C for 30 min.	RP-HPLC
	SSTR[118]	Peptide	Peptide was incubated with NHS ester of CHX-A″-DTPA$(tBu)_5$ glutarate in DMF for 6–8 h at RT, followed by diethyl ether precipitation, deprotection, and RP-HPLC purification.	^{86}Y (in 0.1 M HCl) was incubated with peptide (in 0.5 M NH_4OAc, pH 5.5) at RT for 1 h.	None reported
DOTA	GRPR[223,284,285]	Peptide	Peptide was synthesized *via* standard Fmoc solid phase chemistry. DOTA incorporation method is unclear; however, a tributyl anhydride of DTPA was used for the acylation of prolines in similar DTPA-modified conjugates, so a similar strategy may have been used here.	^{86}Y was incubated with peptide in NH_4OAc (0.5 M, pH 6.5) for 30 min at 80 °C.	RP-HPLC
	MC1-R[219,220,286]	Peptide	Peptide was coupled to DOTA$(tBu)_3$ using an automated peptide synthesizer and standard solid-phase Fmoc chemistry, followed by cleavage from the resin, deprotection, and RP-HPLC purification.	^{86}Y was incubated with peptide in NaOAc (0.1 M, pH 5.5) for 30 min at 85 °C.	RP-HPLC
	SSTR[287,288]	Peptide	A solution of peptide, NHS, and DCC in DMF was added to a solution of DOTA in H_2O, followed by incubation at RT for 24–72 h, deprotection, and RP-HPLC purification.	Peptide in NH_4OAc (0.15 M, pH 4.5, 0.3% BSA) was incubated with ^{86}Y (from α-hydroxyisobutyric acid stock) for 15 min at 100 °C.	RP-HPLC

Chelator	Target	Vector	Conjugation	Radiometallation[a]	Purification
	none (HSA)[119]	Peptide Microspheres	Human serum albumin microspheres were suspended in $Na_2B_4O_7$ (0.1 M, pH not noted) and incubated with *p*-SCN-Bn-DOTA for 24 h at 50 °C, followed by repeated centrifugation and washing steps for purification.	^{86}Y (in 0.04 M HCl) was added to DOTA-HSAM in NH_4OAc (0.5 M, pH 7) and incubated for 15 min at 90 °C at a final pH of 6.5.	Centrifugation

[a]Some protocols call for the use of gentisic acid (typically 1–5 mg mL^{-1}) to protect the biomolecule from radiolysis.

Table 10

Guide to the construction of ^{89}Zr bioconjugates

Chelator	Target	Vector	Conjugation	Radiometallation[a]	Purification
DFO	EpCAM[289] E48 antigen[289]	Antibody	**1** Introduction of maleimide groups to mAb *via* reaction of SMCC[b] in DMF with mAb (in 0.1 M phosphate buffer, pH 8.3) for 30 min at RT **2** Reaction of DFO with SATA to form thioester **3** Incubation of SATA-DFO and freshly prepared hydroxylamine with mAb in phosphate buffer (100 mg mL^{-1}, pH 6.5) for 1 h at RT **4** Purification with size exclusion column	After removal of oxalic acid *in vacuo*, ^{89}Zr solution was added to a solution of mAb (0.1 M NH_4OAc, pH not noted) and incubated for 1 h at RT.	Size exclusion chromatography
	CD44[81,290,291] Met[292] EGFR[293,294] VEGFR[295,296] CD20[297] HER2[298,299]	Antibody	**1** Synthesis of *N*-succinyl-DFO (*N*sucDFO) from DFO mesylate and succinic anhydride **2** Synthesis of Fe(III) *N*sucDFO complex from $FeCl_3$ and *N*sucDFO **3** Formation of activated TFP ester of Fe(III)NsucDFO **4** Incubation of Fe(III)NsucDFO-TFP with mAb for 1 h in carbonate buffer (pH 9.5–10), followed by addition of gentisic acid, and adjustment of pH to 4–4.5 with H_2SO_4 **5** Addition of EDTA (25 mg mL^{-1}) for 30 min at pH 4–4.5 to remove Fe(III) **6** Purification with size exclusion column	Antibody solution (in water, buffer, or sterile saline) was incubated with ^{89}Zr in 0.5 M HEPES buffer for 30–60 min at RT (^{89}Zr originally in 1 M oxalic acid, adjusted to final pH 6.7–7.4 with 2 M Na_2CO_3 and/or 0.5 M HEPES).	Size exclusion chromatography
	CAIX[300,301]	Antibody	Same as immediately above.	Same as above, but with incubation at 37 °C for 60 min.	Size exclusion chromatography
	HER2[302] PSMA[125,303]	Antibody	Same as immediately above.	Antibody solution (in sterile saline) was incubated with ^{89}Zr for 1–2 h at RT (^{89}Zr stock in 1 M oxalic acid adjusted to pH 7.7–8.5 with 1 M Na_2CO_3).	Size exclusion chromatography
	CD44[124,304] EGFR[124] CD20[124]	Antibody	DFO-SCN (in DMSO) was incubated with antibody in $NaHCO_3$ buffer (0.1 M, pH 8.9–9.1) for 30 min at 37 °C, followed by size exclusion chromatography.	Antibody solution was incubated with ^{89}Zr in 0.5 M HEPES buffer for 60 min at RT (^{89}Zr originally in 1 M oxalic acid, adjusted to final pH 6.8–7.2 with 2 M Na_2CO_3 and 0.5 M HEPES)	Size exclusion chromatography
	HER2[305]	Antibody	Thiol-modified antibody was incubated with DFO-Chx-Mal in buffer (50 mM Tris, 150 mM NaCl, pH 7.5) for 1 h at RT, followed by size exclusion chromatography.	Antibody solution was incubated for 1 h at RT with ^{89}Zr solution (originally in 1 M oxalic acid, adjusted to final pH 7.0–8.0, with 2 M Na_2CO_3 and 0.5 M HEPES).	Size exclusion chromatography

Chelator	Target	Vector	Conjugation	Radiometallation[a]	Purification
	HER2[305]	Antibody	Thiol-modified antibody was incubated with DFO-BAC in buffer (0.05 M sodium borate, pH 9.0) for 5 h at RT, followed by size exclusion chromatography.	Same as immediately above	Size exclusion chromatography
	HER2[304,305]	Antibody	Thiol-modified antibody was incubated with DFO-IAC in buffer (50 mM Tris, 150 mM NaCl, 0.0125 M sodium carbonate buffer pH 9) for 2 h at RT, followed by size exclusion chromatography.	Same as immediately above	Size exclusion chromatography

[a] Gentisic acid (typically 1–5 mg mL^{-1}) is often included in metallation solutions to protect against radiolysis.

[b] SMCC = succinimidyl 4-(*N*-maleimdomethyl) cyclohexane-1-carboxylate